OKLAHOMA TRANSPORTATION CENTER

ECONOMIC ENHANCEMENT THROUGH INFRASTRUCTURE STEWARDSHIP

CONTINUOUS REAL TIME MEASUREMENT OF PAVEMENT QUALITY DURING CONSTRUCTION

SESH COMMURI, PH.D.
MUSHARRAH ZAMAN, PH.D.
DHARAMVEER SINGH
ANH MAI
FARES BEAINY

OTCREOS7.1-10-F

Oklahoma Transportation Center
2601 Liberty Parkway, Suite 110
Midwest City, Oklahoma 73110

Phone: 405.732.6580
Fax: 405.732.6586
www.oktc.org

DISCLAIMER

The contents of this report reflect the views of the authors, who are responsible for the facts and accuracy of the information presented herein. This document is disseminated under the sponsorship of the Department of Transportation University Transportation Centers Program, in the interest of information exchange. The U.S. Government assumes no liability for the contents or use thereof.

TECHNICAL REPORT DOCUMENTATION PAGE

1. REPORT NO.	2. GOVERNMENT ACCESSION NO.	3. RECIPIENTS CATALOG NO.
OTCREOS7.1-10-F		

4. TITLE AND SUBTITLE	5. REPORT DATE
Continuous Real Time Measurement of Pavement Quality during Construction	December, 2010
	6. PERFORMING ORGANIZATION CODE
7. AUTHOR(S)	8. PERFORMING ORGANIZATION REPORT
Sesh Commuri, Musharraf Zaman, Dharamveer Singh, Anh Mai, Fares Beainy	
9. PERFORMING ORGANIZATION NAME AND ADDRESS	10. WORK UNIT NO.
The University of Oklahoma 110 W. Boyd Street, DEH 432 Norman, OK 73019	11. CONTRACT OR GRANT NO. DTRT-06-G-00
12. SPONSORING AGENCY NAME AND ADDRESS	13. TYPE OF REPORT AND PERIOD COVERED
Oklahoma Transportation Center (OkTC) (Fiscal) 201 ATRC, Stillwater, OK 74078 (Technical) 2601 Liberty Parkway, Suite 110 Midwest City, Oklahoma 73110	Final June 2009 – October 2010
	14. SPONSORING AGENCY CODE

15. SUPPLEMENTARY NOTES
University Transportation Center

16. ABSTRACT

Intelligent Compaction has been investigated as a means of improving the quality of asphalt pavements during their construction. The long term performance of an asphalt pavement is directly related to its load bearing capability and is determined by the stiffness achieved during the construction process. Early deterioration of pavements due to rutting, fatigue cracking and other types of distresses can be traced to inadequate stiffness. While dependence of pavement performance on stiffness is well known, this parameter is rarely measured during construction of the pavements. Instead, current quality control in the field during the construction of asphalt pavements focuses on the measurement of density of the finished pavement at specific locations.

In this research project, the use of OU's Intelligent Asphalt Compaction Analyzer (IACA) in determining the modulus of the entire pavement under construction is demonstrated. The ability to continuously monitor the modulus of the pavement will help identify and address improper compaction during construction. Low stiffness resulting from inadequate compaction can be addressed while the asphalt mat is still hot and pliable thereby leading to longer lasting roads. The IACA-based approach for estimating the stiffness of the pavement during construction is shown to be a cost effective technique for assessing the quality, and it provides a means to improve the overall quality of asphalt pavements during construction.

17. KEY WORDS	18. DISTRIBUTION STATEMENT		
Asphalt Pavements, Intelligent Compaction, Dynamic Modulus	No restrictions. This publication is available at www.oktc.org and from the NTIS.		
19. SECURITY CLASSIF. (OF THIS REPORT)	20. SECURITY CLASSIF. (OF THIS PAGE)	21. NO. OF PAGES	22. PRICE
Unrestricted	Unrestricted	79 pages + covers	

ACKNOWLEDMENTS

The field demonstration reported in this report would not have been possible without the unparalleled support of Haskell Lemon Construction Company (HLCC), Oklahoma City, Oklahoma. Access to HLCC's construction sites and equipment as well as their technical staff has been vital to the success of this project. In particular, the authors wish to thank Jay Lemon, Chief Executive Officer, HLCC and Bob Lemon, Chief Operations Officer, HLCC for their vision and unqualified support of the research team. HLCCs partnership with OU has been critical for the success of this project.

The authors also wish to acknowledge the financial support of Oklahoma Transportation Center. The financial support of and technical partnership with Volvo Construction Equipment (VCE), Shippensburg, PA are duly acknowledged. The assistance of Burgess Engineering, Moore, Oklahoma in conducting spot tests for pavement quality is also greatly appreciated.

SI (METRIC) CONVERSION FACTORS

Approximate Conversions to SI Units

Symbol	units	Multiply by	To Find	Symbol
LENGTH				
in	inches	25.40	millimeters	mm
ft	feet	0.3048	meters	m
yd	yards	0.9144	meters	m
mi	miles	1.609	kilometers	km
AREA				
in^2	square inches	645.2	square millimeters	mm^2
ft^2	square feet	0.0929	square meters	m^2
yd^2	square yards	0.8361	square meters	m^2
ac	acres	0.4047	hectares	ha
mi^2	square miles	2.590	square kilometers	km^2
VOLUME				
fl oz	fluid ounces	29.57	milliliters	mL
gal	gallons	3.785	liters	L
ft^3	cubic feet	0.0283	cubic meters	m^3
yd^3	cubic yards	0.7645	cubic meters	m^3
MASS				
oz	ounces	28.35	grams	g
lb	pounds	0.4536	kilograms	kg
T	short tons (2000 lb)	0.907	megagrams	Mg
TEMPERATURE (exact)				
°F	degrees Fahrenheit	(°F-32)/1.8	degrees Celsius	°C
FORCE and PRESSURE or STRESS				
lbf	poundforce	4.448	Newtons	N
lbf/in^2	poundforce per square inch	6.895	kilopascals	kPa

Approximate Conversions from SI Units

Symbol	units	Multiply by	To Find	Symbol
LENGTH				
mm	millimeters	0.0394	inches	in
m	meters	3.281	feet	ft
m	meters	1.094	yards	yd
km	kilometers	0.6214	miles	mi
AREA				
mm^2	square millimeters	0.00155	square inches	in^2
m^2	square meters	10.764	square feet	ft^2
m^2	square meters	1.196	square yards	yd^2
ha	hectares	2.471	acres	ac
km^2	square kilometers	0.3861	square miles	mi^2
VOLUME				
mL	milliliters	0.0338	fluid ounces	fl oz
L	liters	0.2642	gallons	gal
m^3	cubic meters	35.315	cubic feet	ft^3
m^3	cubic meters	1.308	cubic yards	yd^3
MASS				
g	grams	0.0353	ounces	oz
kg	kilograms	2.205	pounds	lb
Mg	megagrams	1.1023	short tons (2000 lb)	T
TEMPERATURE (exact)				
°C	degrees Celsius	9/5+32	degrees Fahrenheit	°F
FORCE and PRESSURE or STRESS				
N	Newtons	0.2248	poundforce	lbf
kPa	kilopascals	0.1450	poundforce per square inch	lbf/in^2

CONTINUOUS REAL TIME MEASUREMENT OF PAVEMENT QUALITY DURING CONSTRUCTION

Research Project

Sesh Commuri[†]
Associate Professor

Musharraf Zaman[††]
David Ross Boyd Professor
Aaron Alexander Professor
Associate Dean for Research and Graduate Programs

Dharamveer Singh[†††], **Anh Mai**[†], **Fares Beainy**[†]

[†]School of Electrical and Computer Engineering
The University of Oklahoma
110 W. Boyd, Street, DEH 432
Norman, Oklahoma 73019

[††]College of Engineering
The University of Oklahoma
202 W. Boyd, Street, CEC 106
Norman, Oklahoma 73019

[†††]School of Civil Engineering and Environmental Sciences
The University of Oklahoma
202 W. Boyd, Street, CEC 334
Norman, Oklahoma 73019

Oklahoma Transportation Center
2601 Liberty Parkway, Suite 110
Midwest City, Oklahoma 73110

TABLE OF CONTENTS

LIST OF FIGURES

LIST OF TABLES

1. EXECUTIVE SUMMARY

One of the goals of the mechanistic design of asphalt pavements is to address their long term performance. The stiffness of the pavement is a key factor in the design as it directly impacts the load bearing capability of the road. Further, early deterioration of pavements due to rutting or fatigue cracking can be traced to inadequate stiffness. While the dependence of pavement performance on stiffness is well known, this parameter is rarely measured during construction of pavements. Instead, current quality control in the field during construction of asphalt pavements focuses on the measurement of density of the finished pavement at specific locations. Intelligent Compaction techniques in the future will have to have the ability to estimate the modulus of the pavement continuously during its construction. The goal of this project is to extend OU's Intelligent Asphalt Compaction Analyzer (IACA) to determine the modulus of the entire pavement in real-time during its construction.

The IACA is a roller mountable device that can sense the vibrations of the roller during the compaction of a pavement and using the knowledge of the asphalt mix and the pavement design, can estimate the achieved level of compaction of the asphalt mix. The IACA technology was developed during 2003-2006 with support from the Oklahoma Center for the Advancement of Science and Technology (OCAST). During 2006-2009[†], the use of the IACA to determine the density of asphalt pavements was demonstrated during the construction of asphalt pavements across the United States. The results of these tests showed that the IACA was able to estimate the density of the pavement during its construction to within $\pm 1.5\%$ of the actual density. This accuracy is comparable to the measurement accuracy of spot density measurement tools currently being used by the paving industry and by the transportation agencies such as Oklahoma Department of Transportation (ODOT). However, the IACA additionally provides instantaneous complete coverage of the pavement which can help in the elimination of over/ under compaction of the pavement.

In order to extend the capability of the IACA to measure stiffness of hot mix asphalt during its compaction, properties of different asphalt mixes were first studied in the laboratory.

[†]Development of IACA Prototype, Assistance Grant # DTFH61-08-G-0002, Highways for LIFE Technology Partnerships Program, Federal Highway Administration, US Department of Transportation, Washington, DC, 2008-10. Also, Grant # OU 105-070800 and OU 105-127800 from Volvo Construction Equipment (VCE), Shippensburg, PA.

The variation of dynamic modulus of compacted mixes was studied as a function of the degree of compaction, temperature, loading frequency, and mix parameters. The dynamic modulus master curves that were developed were then used to calibrate the IACA. The performance of the calibrated IACA was tested during construction of Interstate I-35 in Norman, OK. The estimated modulus over the entire pavement section was recorded during each roller pass. This data was then used to generate the modulus of the completed pavement. After the construction, the pavement was allowed to cool down to ambient temperature and Falling Weight Deflectometer (FWD) tests were conducted at 25 locations approximately 5 meters apart on the center of the compacted lane. The results obtained during field compaction were found to be in good agreement with FWD measurements from the completed pavement.

The laboratory studies that were conducted as part of this research indicate that modulus values determined through laboratory testing of compacted specimen are significantly higher than the modulus values observed during field compaction. While these empirical models can be used to estimate the stiffness of different asphalt mixes with reasonable accuracy, their performance depends on the design of the mix and correction factors have to be determined prior to their use. Validated empirical models can then be used to predict the performance of the asphalt mixes and minimize the need for conducting costly dynamic modulus tests in the laboratory.

The results of this project also demonstrate that the IACA can estimate the stiffness of the pavement during its construction and can serve as a quality control tool. Identification of under-compacted areas while the asphalt mix is hot and pliable will enable the paving crew to perform additional compaction at these locations. The real-time measurement of stiffness will also help avoid over-compaction of a pavement. The estimated stiffness can be verified through non destructive tests after the construction of the pavement. Such testing will help reduce the need for destructive testing like coring during the quality assurance process.

Research is underway to test the functioning of the IACA at several construction sites across Oklahoma. The effect of the subgrade, asphalt mix, thickness of the pavement layer on the accuracy of the stiffness estimates is being investigated under a research grant from our industry sponsor, VCE. An application for a patent has been filed with the United States Patent and Trademark Office to protect the technology developed in this project. This technology has been licensed to VCE and is likely to be commercially available in late 2013.

2. PROBLEM STATEMENT

Stiffness is a key design factor that directly impacts the load bearing capacity of roadway pavements. Early deterioration of pavements due to rutting, fatigue cracking, and other types of distresses may be attributed to inadequate stiffness achieved during the compaction process (Pellinen and Witczak, 2002). The stiffness of the pavement is typically expressed in terms of its modulus, i.e., the relationship between the applied stress and the resulting deformation. While there are several ways to define stiffness of a HMA layer, dynamic modulus of hot-mix asphalt (HMA) is selected as one of the fundamental inputs in the mechanistic-empirical pavement design guide (MEPDG) (NCHRP, 2004). The National Cooperative Highway Research Program (NCHRP) Project I-37A recommends the use of dynamic modulus to characterize the HMA mixes (AASHTO, 2002).

Failure to achieve the desired stiffness during the construction of the pavement is a leading cause for early degradation of asphalt pavements. Excessive rutting, cracking, potholes etc., that are signs of failure of asphalt pavements can be avoided by using good quality control tools during the compaction process and through the adoption of better construction practices. Unfortunately, the stiffness of a pavement is seldom measured during its construction. Instead, the current quality control (QC) methods focus on the measurement of density of the finished pavement at specific locations. The most reliable method of measuring pavement density is the extraction of cores at several locations on the finished pavement and conducting air voids tests in the laboratory as specified in AASHTO T166 (AASHTO, 2006). This method of testing, however, is time consuming, costly, and destructive. Alternative methods for in-place measurement of density of hot mix asphalt (HMA) layers include the use of both nuclear density gauges and non-nuclear density gauges. The nuclear-based devices tend to have problems associated with licensing, equipment handling, and storage. In addition, both of these technologies allow only point-wise measurements of density during the construction of an asphalt pavement. These manual processes of measurement are time consuming and result in avoidable delays in the construction while not reflecting the overall quality of the pavement.

2.1 IMPORTANCE OF THE PROBLEM

There are over 4 million miles of pavements in the United States (FHWA, 2005). Almost 2.2 million miles (55%) of these pavements are paved with asphalt. In the United States, over 550 million tons of hot mix asphalt (HMA) are produced and placed each year. The total expenditures for asphalt pavement surfaces are in excess of $25 billion annually and over

300,000 men and women are employed in the asphalt industry (FHWA, 2007).

While the level of government spending on road construction and repair has increased steadily in recent years, deterioration of existing roadways has also been increasing at an alarming rate. At present, twenty-six percent of the nation's major metropolitan roads – interstates, freeways and other critical local routes – have pavements in poor condition, resulting in rough rides and costing the average urban motorist $383 annually in additional vehicle operating costs due to accelerated vehicle deterioration, additional maintenance needs and increased fuel consumption (Moretti, 2005). Some of this can be directly attributed to the increase in vehicular traffic nationwide. For example, during 1991 to 2001, vehicle travel on Oklahoma highways increased by 27%, while state's population grew by only 10% during the same period (FHWA, 2005). Conservative estimates indicate a 33% increase in cars on highways and 70% increase in trucks over the next 20 year (FHWA, 2006; OAPA, 2003).Trucks would also be carrying about 50 percent more weight in the next decade, according to the American Trucking Association. A 1979 federal study estimates that the damage done by one truck is equivalent to the damage caused by 9,600 cars. With increased axle loads in trucks, the damage is expected to be much worse today. These statistics are representative of the problem nation-wide (FHWA, 2006).

According Oklahoma Asphalt Pavement Association, there are between 110 and 120 active asphalt contractors in the state. Of those, about 20 companies undertake about 80% of all the work. Some contractors work on subdivisions, while others work on major projects involving highways, Interstates, turnpikes, county roads, etc., consisting of multiple miles at a time. Cost of each of these projects can range anywhere from $500,000 to millions of dollars. While the large construction projects typically require the paving of as many as 15-20 miles at a time, they also carry some of the stiffest penalties if smoothness and compaction levels are not met. These penalties can range from 5% to 50% of the contract. This puts a strain on contractors to do the best work possible and causes reduction in productivity.

Therefore, there is an immediate need to develop cost-effective technique that will provide a clear and complete account of the quality of the pavement being constructed. Rapid in situ stiffness testing will enable the development of reliable and verifiable quality assurance programs. In addition to lowering the cost of construction and maintenance of the asphalt roads, these programs will result in longer lasting roads and will help relate test results to design practice.

2.2 STATE-OF-THE-ART

In-situ testing of mechanical properties of pavements and underlying subgrade soils is a widely researched area. Several test devices such as the Benkelman Beam, Lacroix Deflectograph, static plate loading test, and Falling Weight Deflectometer (FWD) are available for nondestructive evaluation of asphalt pavements (Newcomb and Birgisson, 1999; Tayabji and Lukanen, 2000). More recently, the rolling weight deflectometer, spectral analysis of surface waves, and the Humboldt stiffness gauge have also been used to measure in-situ stiffness of pavement layers including subgrade (Newcomb and Birgisson, 1999; Navaratnarajah, 2006). However, these test devices are applicable only after the compaction process is complete and pavement has cooled down to the ambient temperature. Therefore, although these tools can be used to identify deficiencies in compaction, they are not suitable for use during the construction of the pavement.

With increased emphasis on the new mechanistic-empirical (M-E)-based design procedures, predictive equations have been developed to estimate dynamic modulus of HMA layers as a function of such properties as mix type, aggregate structure, binder specifications, volumetric properties of compacted specimens, and mix temperature (Andrei et al., 2002; Ayres et al., 1998; Crovetti et al., 2005; Katicha, 2003; Tarefder, 2003). While these tests are adequate to study the properties of the asphalt mix in the laboratory, they too are not suitable for determining the stiffness of the pavement during its construction.

The need to measure the stiffness of a pavement during construction has motivated the industry and equipment manufacturers to develop technologies that can ensure consistent and optimal compaction of HMA pavements (Camargo et al. 2006; Landers, 2006; Moore 2006; Peterson 2005). Uniform compaction of both soil and aggregate bases is achieved through the variation of machine parameters such as amplitude and frequency of vibrations, and vectoring of the thrust. Dynamic control of machine parameters allows for the application of vibratory energy only to under-compacted areas and thereby preventing over-compaction and ensuring uniform compaction of subgrade soils and/or aggregate bases. While these intelligent compaction (IC) techniques hold promise, their performance is still being evaluated by several Departments of Transportations (DOTs) and the Federal Highway Administration (FHWA) (FHWA, 2011).

In contrast to the aforementioned intelligent compaction (IC) technologies (Ammann, Asphalt Manager, Caterpillar, Asphalt Compaction, Sakai), the Intelligent Asphalt Compaction

Analyzer (IACA) (Commuri et al. 2008; Commuri et al. 2009a; Commuri et al. 2009b, Commuri and Zaman, 2010) is a measurement tool that analyzes, in real time, the vibrations of a vibratory compactor to estimate the level of compaction of a HMA mat or layer during construction. Use of IACA to estimate the density of asphalt pavements during construction was demonstrated during actual construction of asphalt pavements (Commuri, 2011).

2.3 PROJECT GOALS, TASKS, AND ANTICIPATED OUTCOMES

The primary goal of this project is the extension of the IACA for continuous measurement of the stiffness (dynamic modulus) of an asphalt pavement during its construction. The technology represents a fundamental shift from the density measurement as a Quality Assurance/Quality Control (QA/QC) method to QA/QC methods based on mechanistic properties. The following steps are designed in order to meet this objective.

Step 1. Investigate the dependence of the dynamic modulus of compacted asphalt specimen on the various parameters in the asphalt mix.

Step 2. Develop dynamic modulus master curves as a function of temperature, loading frequency, and air voids in the compacted specimen.

Step 3. Determine the target dynamic modulus values for a given pavement layer. Develop calibration techniques for the IACA to estimate the modulus of the pavement at 21^0C and 5 Hertz loading frequency.

Step 4. Verify the estimated stiffness of each pavement layer by conducting Falling Weight Deflectometer (FWD) tests on the completed pavement.

Deliverables include (a) procedures for measuring the modulus of asphalt pavement layers; (b) procedure for preparing test specimen and determining the master curves for the dynamic modulus; (c) calibration procedure for the IACA; and (d) final report including field validation data demonstrating the ability of the IACA to continuously measure the stiffness of the compacted pavement.

It is anticipated that the IACA will provide continuous, instantaneous measurement of the stiffness of each layer of the pavement during the construction process. As built maps generated by the IACA after the completion of the construction will provide a clear and complete account of the quality of the pavement. The proposed innovation will lead to lower cost and

better quality evaluations of pavement characteristics and result in quality control programs that relate test results to design practice.

2.4 ORGANIZATION OF THE REPORT

The rest of this report is organized as follows. The measurement of the dynamic modulus in the laboratory is discussed in Section 3. Since the measurement of the dynamic modulus is time consuming and requires the use of specialized equipment, MEPDG allows for the estimation of the dynamic modulus using empirical models. In Section 4, four different empirical models that are commonly used in Level 2 and Level 3 of MEPDG are evaluated. The performance of these empirical models in predicting the behavior of asphalt mixes that are commonly used in Oklahoma is also presented. The background on the IACA and the calibration procedure to estimate the stiffness in discussed in Section 5. The use of the calibrated IACA during the construction of asphalt pavements is then demonstrated. The report concludes with a summary of the results, and a discussion on technology transfer and direction of future research.

3. MEASUREMENT OF STIFFNESS OF ASPHALT MIXES IN THE LABORATORY

The long term performance of a pavement depends to a large extent on the properties of the materials constituting the asphalt mix. Several researchers have reported that the dynamic modulus (|E*|) of a HMA mix is highly correlated to pavement distresses (i.e., rutting, fatigue, and low temperature cracking) over a wide range of traffic and climatic conditions (Goh et al., 2011; Loulizi et al., 2006; Bonaquist, 2003; Pellinen et al., 2002; Shenoy et al., 2002; Witczak et al., 2002; Cominsky et al., 1998). A high |E*| (high stiffness) improves the load carrying ability of asphalt layers and reduces the stress-strain on the underlying layers. However, excessive stiffness can reduce the durability of the pavement and increase the possibility of thermal cracking in surface layers. On the other hand, low |E*| (low stiffness) decreases the load bearing capacity and could possibly result in the rutting failure of the pavement. Therefore, an accurate estimation of |E*| is important for designing a structurally sound pavement. In this section, the measurement of the dynamic modulus in the laboratory is presented.

3.1 DETERMINATION OF THE DYNAMIC MODULUS IN THE LABORATORY

A dynamic modulus master curve for asphalt concrete is a critical input in the design of flexible pavements. The recommended testing to develop the modulus master curve is presented in AASHTO Provisional Standard TP62-03, Standard Method of Test for Determining Dynamic Modulus of Hot-Mix Asphalt Concrete Mixtures. Selection of asphalt mix, preparation of test specimens, and determination of dynamic modulus of compacted specimens are discussed below. The test data is then used to generate dynamic modulus master curves.

3.2 MATERIAL SELECTION

Five different types of loose hot mix asphalt (HMA) that are commonly used in Oklahoma were collected from Haskell Lemon Plant in Norman. The mixes varied from 19 mm nominal maximum aggregate size to 12.5 mm nominal maximum aggregate size and included three different types of binders (PG 64-22, PG70-28, and PG 76-28). Three of the five mixes also contained recycled asphalt pavement (RAP). These asphalt mixes are representative of the mixes typically used in Oklahoma. The description of the mixes is given below. Table 3.1 shows the gradation of the all five mixes.

Mix-1: The nominal maximum aggregate size was 19 mm. The mix contained approximately 20 percent 1” #67 rock, 44 percent manufactured sand, 11 percent sand, and 25 RAP, with 4.1 percent PG 64-22 OK binder.

Mix-2: The nominal maximum aggregate size was 19 mm. The mix contained approximately 22 percent 1” #67 rock, 50 percent manufactured sand, 13 percent sand, and 15 percent RAP, with 4.1 percent PG 76-28 OK binder.

Mix-3: The nominal maximum aggregate size was 12.5 mm. The mix contained approximately 38 percent 5/8” chips, 27 percent manufactured sand, 24 percent C-33 screening, and 11 percents sand, with 4.5 percent PG 70-28 OK binder.

Mix-4: The nominal maximum aggregate size was 12.5 mm. The mix contained approximately 25 percent 5/8” chips, 38 percent manufactured sand, 22 percent screening, and 15 percents sand, with 5.1 percent PG 64-22 OK binder.

Mix-5: The nominal maximum aggregate size was 12.5 mm. The mix contained approximately 22 percent 5/8” chips, 23 percent manufactured sand, 20 percent C-33 screening, 10 percent screening, 10 percents sand, and 15 percent RAP with 4.2 percent PG 76-28 OK binder.

Table 3.1 Aggregate Gradation of all Five Mixes

Gradation	Mix Type				
(%Passing)	Mix-1	Mix-2	Mix-3	Mix-4	Mix-5
Sieve size (mm)					
25	100	100			
19	98	98	100	100	100
12.5	87	87	97	98	98
9.5	80	80	89	87	87
4.75	58	62	69	62	62
2.36	37	40	49	40	40
1.18	25	27	35	28	28
0.6	19	20	25	21	21
0.3	12	12	15	13	13
0.15	4	5	7	5	5
0.075	2.9	2.8	2.5	3.2	3.2
Aggregate Type	Limestone	Limestone	Granite	Rhyolite	Limestone
Mix Type	Recycled	Recycled	Virgin	Virgin	Recycled

3.3 PREPARATION OF TEST SPECIMEN

Specimens were compacted using a Superpave® Gyratory Compactor (SGC) at 6, 8, 10, and 12% target air voids (± 0.5%). These air voids were selected as they are representative of the

practical range of compaction density (i.e., 94% to 88% of the theoretical maximum density) encountered during the construction of a flexible pavement. Three replicate of specimens were compacted at each level of air void. First, specimens having 150 mm diameter by 167.5 mm height were prepared. Then, the test specimens of size 100 mm in diameter and 150 mm height were cored and sawed from the center of the gyratory compacted specimens (Figure 3.1). These specimens have the most consistent air voids distribution in both vertical and radial directions (Chehab et al., 2000). Moreover, these are the specimen geometries currently recommended for the simple performance test and used in constitutive modeling of asphalt concrete in tension and compression (Chehab et al., 2002; Schwartz et al., 2002; Witczak et al., 2002; Daniel, 2001). Volumetric analyses were conducted to obtain effective binder content (V_{beff}), voids in mineral aggregates (VMA), voids filled with asphalt (VFA), and air voids (V_a) for both the mixes (Table 3.2).

3.4 TEST PROCEDURE

Dynamic modulus values were measured in the laboratory in accordance with AASHTO TP62-03 specification (AASHTO, 2006). All tests were performed using a MTS servo-hydraulic testing system. Each mix was tested for different levels of air voids, as mentioned above. The test was conducted on each test specimen at four different temperatures: 4, 21, 40, and 55^{o}C, and six different frequencies: 25, 10, 5, 1, 0.5, and 0.1 Hz. The test specimen was placed in an environmental chamber and allowed to reach equilibrium within ±0.5^{o}C of the specified test temperature. The temperature of the specimen was monitored using a dummy specimen with a thermocouple mounted at the center. The deformation of the specimen was measured using two linear variable differential transducers (LVDTs) mounted on the specimen. The LVDTs were adjusted to operate to near the end of their linear range to allow the full range to be available for the accumulation of compressive permanent deformation. To reduce the friction, teflon papers were placed between the specimen ends and loading plates. Prior to testing, the specimen was conditioned by applying 200 cycles of load at a frequency of 25 Hz. The load magnitude was adjusted based on the material stiffness, air void content, temperature, and frequency to keep the strain response within 50-150 micro-strains (Tran et al., 2006). Figure 3.2 shows dynamic modulus testing in progress.

Figure 3.1 Preparation of Test Specimen in the Laboratory

Figure 3.2 Dynamic Modulus Test in Progress

Table 3.2 Volumetric Properties of Mixes

		Mix-1	Mix-2	Mix-3	Mix-4	Mix-5
G_{mm}		2.505	2.523	2.463	2.477	2.508
G_{se}		2.671	2.677	2.658	2.681	2.688
G_{sb}		2.645	2.657	2.634	2.669	2.652
G_b		1.01	1.01	1.01	1.02	1.01
Binder Type		PG 64-22	PG 76-28	PG 70-28	PG 64-22	PG 76-28
P_b (%)		4.1	4.1	4.5	5.1	4.2
VMA (%)	Min.	14.11	14.81	16.23	16.6	14.95
	Max.	20.42	20.11	21.55	22.12	20.59
VFA (%)	Min.	39.88	42.86	41.37	47.71	39.24
	Max.	62.21	62.04	58.77	68.09	57.87

G_{mm} = Maximum Theoretical Specific Gravity Mixture
G_{se} = Effective Sp.Gr. of Aggregate
G_{sb} = Bulk Specific Gravity of Aggregate
G_b = Specific Gravity of Binder
V_a = Air Voids
VMA = Voids in Mineral Aggregates
VFA = Voids Filled with Asphalt
T (C) = Temperature
P_b = Binder Content

3.5 CONSTRUCTION OF THE MASTER CURVES

Master curves were generated at a reference temperature of 21^{o}C using the procedure outlined in Bonaquist et al., (2005). This procedure eliminates the lower temperature requirement, so that time required in conducting |E*| testing and master curve construction can be reduced. The limiting maximum modulus is estimated based on binder stiffness and mix volumetric data using the Hirsch model (Christensen et al., 2003). Equations (3.1) and (3.2) show the sigmoidal function and shift factor used for fitting the master curve. The default value of 'A' and 'VTS' for the different binder was taken from AASHTO. A nonlinear optimization program was used for simultaneously solving these unknown parameters.

$$\log|E^*| = \delta + \frac{(\text{Max} - \delta)}{1 + e^{\beta+\gamma\left[\log(f)+c\left(10^{(A+VTS\log T_R)}-\log\eta_{t=r}\right)\right]}} \quad (3.1)$$

$$a(T) = \frac{f_r}{f} \quad (3.2)$$

where, Max is the maximum E* for a particular mix, f_r is the reduced frequency at reference temperature, f is the frequency at a particular temperature, $\eta_{t=r}$ is the viscosity of binder at reference temperature, A is the regression intercept of viscosity-temperature curve, VTS is the regression slope of viscosity-temperature susceptibility, $\alpha(T)$ is the shift factor as a function of

temperature and age, and δ ,β, γ, c are fitting parameters. Figures 3.3 through 3.7 shows the typical master curve constructed for all five mixes, and Tables 3.3 - 3.7 list the master curves parameters for these mixes.

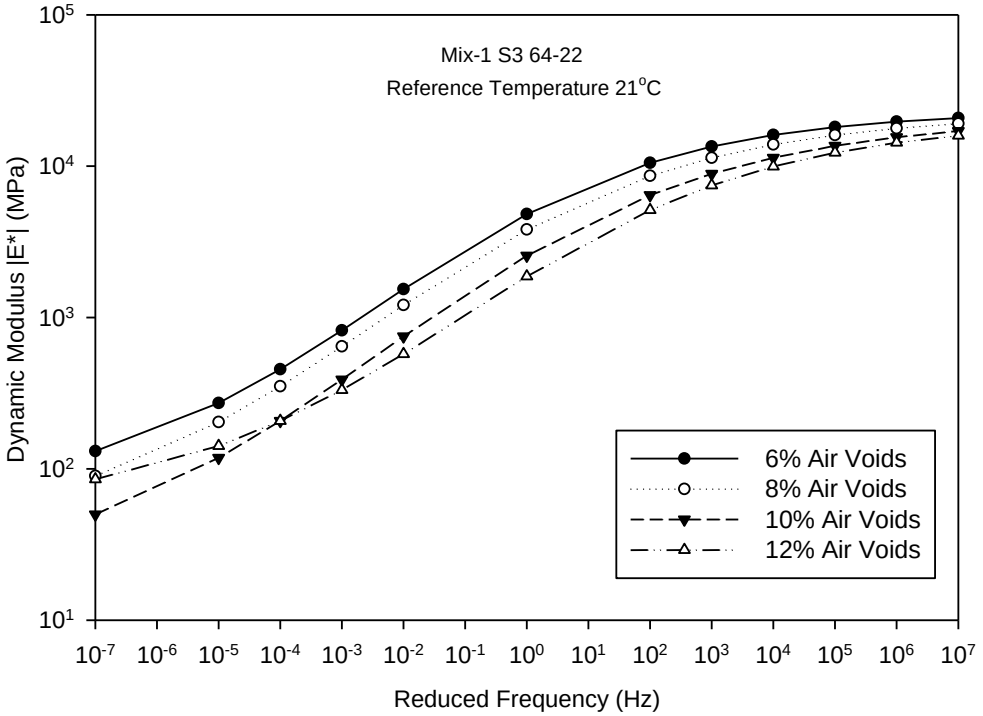

Figure 3.3 Master Curves for Mix-1 (S3 64-22)

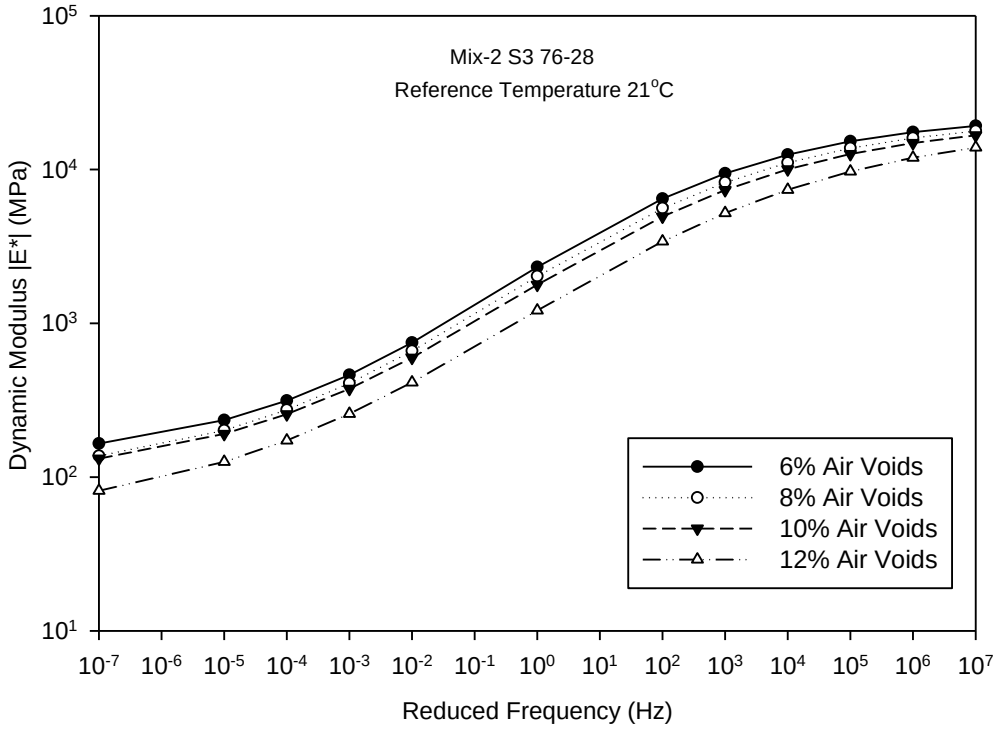

Figure 3.4 Master Curves for Mix-2 (S3 76-28)

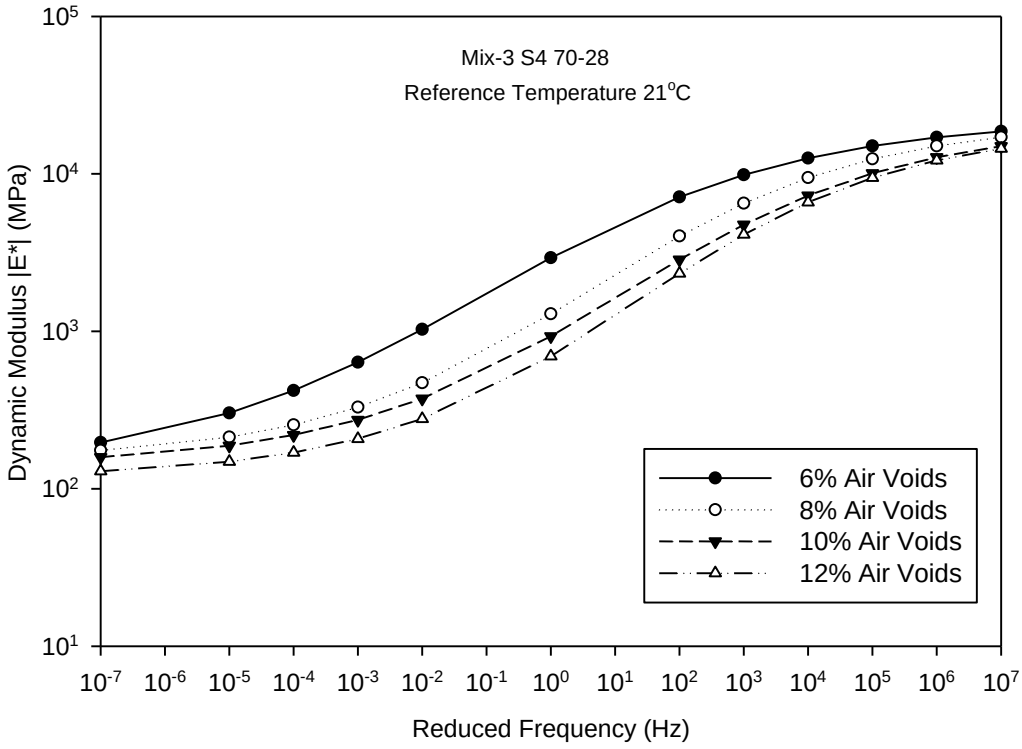

Figure 3.5 Master Curves for Mix-3 (S4 70-28)

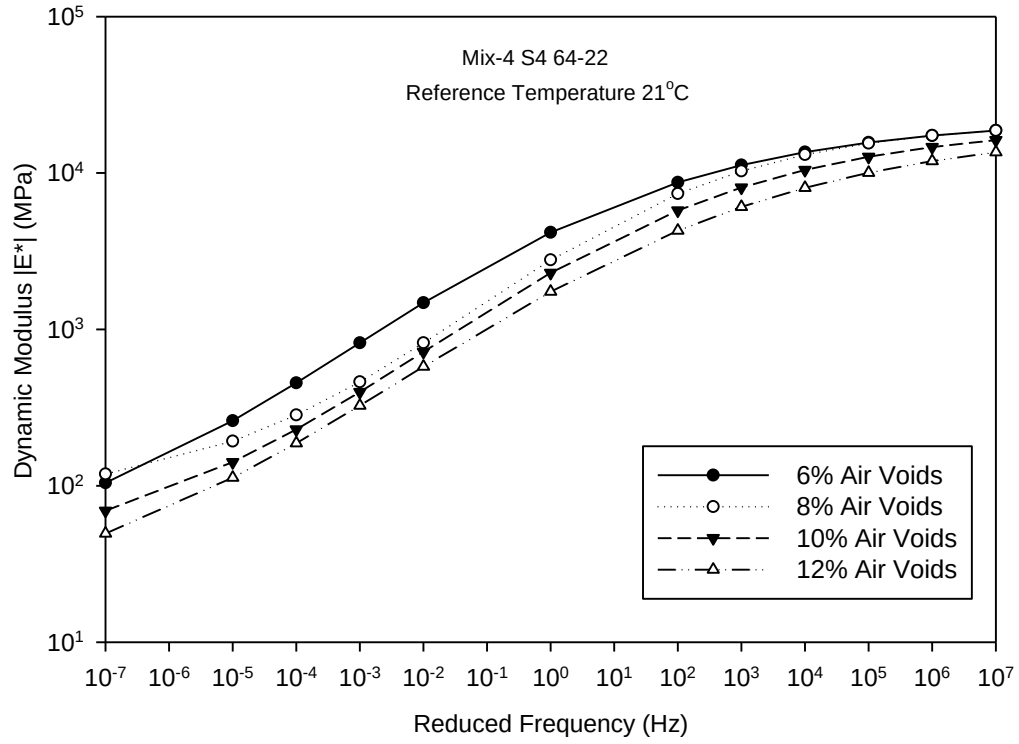

Figure 3.6 Master Curves for Mix-4 (S4 64-22)

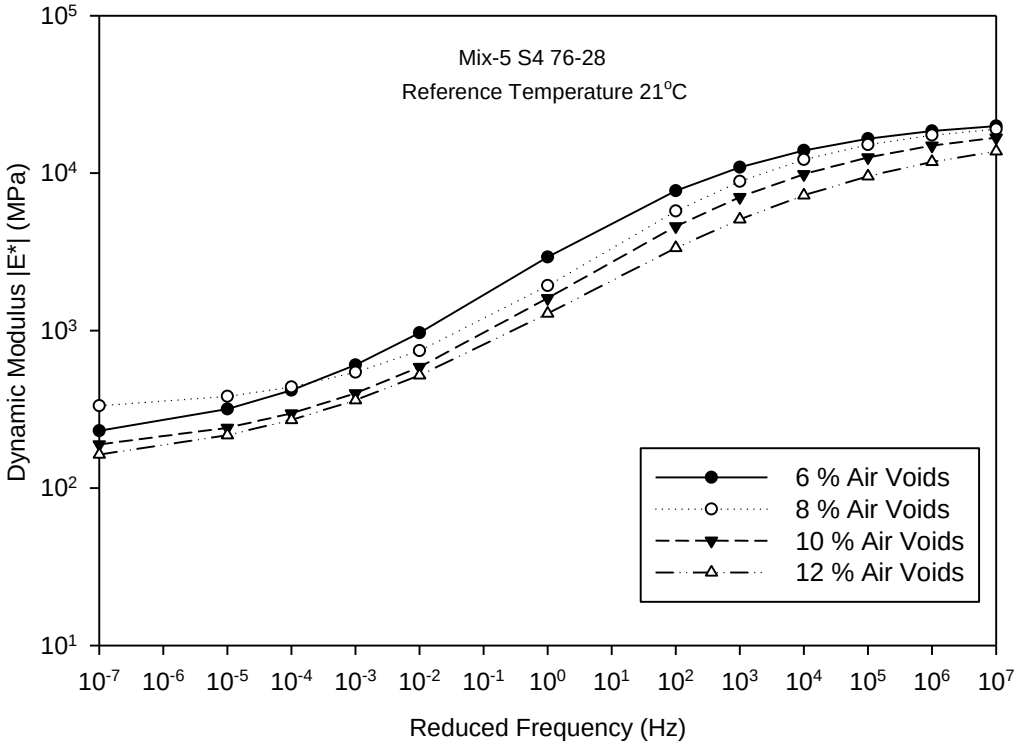

Figure 3.7 Master Curves for Mix-5 (S4 76-28)

Table 3.3 Master Curve and Shift Factor Parameter for Mix-1 (S3 64-22)

Mix-1 (S3 64-22)								
Air Voids (%)	Max E* (MPa)	δ	β	γ	c	R^2	S_e/S_y	Fit
6	23084	1.81	-1.02	-0.43	1.20	0.99	0.07	Excellent
8	22256	1.54	-0.98	-0.39	1.20	0.99	0.05	Excellent
10	21232	1.23	-0.86	-0.37	1.04	0.99	0.06	Excellent
12	19942	1.72	-0.41	-0.40	1.05	0.99	0.08	Excellent

Shift Factors log(aT)

Air	Mix-1 (S3 64-22)			
Voids (%)	4° C	21° C	40° C	55° C
6	2.66	0.00	-2.23	-3.60
8	2.65	0.00	-2.22	-3.58
10	2.30	0.00	-1.93	-3.11
12	2.32	0.00	-1.95	-3.14

Table 3.4 Master Curve and Shift Factor Parameter for Mix-2 (S3 76-28)

Mix-2 (S3 76-28)								
Air Voids (%)	Max E* (MPa)	δ	β	γ	c	R^2	S_e/S_y	Fit
6	22826	2.10	-0.25	-0.45	1.24	0.99	0.04	Excellent
8	22027	1.99	-0.24	-0.42	1.18	0.99	0.05	Excellent
10	21157	1.98	-0.17	-0.42	1.12	0.99	0.04	Excellent
12	20182	1.71	-0.12	-0.37	1.13	0.99	0.05	Excellent

Shift Factors log(aT)				
Air	Mix-2 (S3 76-28)			
Voids (%)	4° C	21° C	40° C	55° C
6	2.24	0.00	-1.96	-3.20
8	2.13	0.00	-1.86	-3.04
10	2.02	0.00	-1.77	-2.89
12	2.04	0.00	-1.78	-2.91

Table 3.5 Master Curve and Shift Factor Parameter for Mix-3 (S4 70-28)

Mix-3 (S4 70-28)								
Air Voids (%)	Max E* (MPa)	δ	β	γ	c	R^2	S_e/S_y	Fit
6	22224	2.12	-0.43	-0.41	1.17	1.00	0.07	Excellent
8	21401	2.19	0.28	-0.47	1.12	0.99	0.09	Excellent
10	20367	2.15	0.49	-0.46	1.05	1.00	0.05	Excellent
12	19562	2.07	0.63	-0.49	1.04	0.99	0.06	Excellent

Shift Factors log(aT)				
Air	Mix-3 (S4 70-28)			
Voids (%)	4° C	21° C	40° C	55° C
6	2.21	0.00	-1.91	-3.10
8	2.12	0.00	-1.83	-2.98
10	1.99	0.00	-1.72	-2.80
12	1.96	0.00	-1.70	-2.76

Table 3.6 Master Curve and Shift Factor Parameter for Mix-4 (S4 64-22)

Mix-4 (S4 64-22)								
Air Voids (%)	Max E* (MPa)	δ	β	γ	c	R^2	S_e/S_y	Fit
6	22367	1.45	-1.09	-0.36	1.29	1.00	0.05	Excellent
8	21481	1.90	-0.55	-0.45	1.15	1.00	0.04	Excellent
10	20715	1.46	-0.69	-0.37	1.20	1.00	0.04	Excellent
12	19851	1.12	-0.70	-0.32	1.15	0.99	0.07	Excellent

Shift Factors log(aT)				
Air	Mix-4 (S4 64-22)			
Voids (%)	4° C	21° C	40° C	55° C
6	2.86	0.00	-2.41	-3.87
8	2.54	0.00	-2.13	-3.44
10	2.65	0.00	-2.23	-3.59
12	2.55	0.00	-2.14	-3.45

Table 3.7 Master Curve and Shift Factor Parameter for Mix-5 (S4 76-28)

Mix-5 (S4 76-28)								
Air Voids (%)	Max E* (MPa)	δ	β	γ	c	R^2	S_e/S_y	Fit
6	22632	2.26	-0.30	-0.47	1.05	0.99	0.05	Excellent
8	21675	2.49	0.28	-0.53	1.07	1.00	0.04	Excellent
10	21020	2.20	0.10	-0.45	0.96	1.00	0.06	Excellent
12	19842	2.09	0.16	-0.39	0.96	1.00	0.08	Excellent

Shift Factors log(aT)				
Air	Mix-5 (S4 76-28)			
Voids (%)	4° C	21° C	40° C	55° C
6	1.91	0.00	-1.67	-2.73
8	1.93	0.00	-1.69	-2.76
10	1.74	0.00	-1.53	-2.49
12	1.74	0.00	-1.52	-2.49

3.6 EXPERIMENTAL RESULTS AND OBSERVATIONS

3.6.1 Effects of Air Voids on Dynamic Modulus

It was seen that as the air voids in the compacted specimen increased, the dynamic modulus of HMA mixes decreased for all combinations of test frequency and temperature. The maximum dynamic modulus was observed at 6% air voids, and it decreased by a factor of 2-4 at 12% air voids depending upon the type of mix.

3.6.2 Effects of Temperature on Dynamic Modulus

The dynamic modulus decreases exponentially with increase in temperature. This exponential relationship between temperature and dynamic modulus was observed for all types of mixes considered in this study.

3.6.3. Effects of Gradation on Dynamic Modulus

Mix-2 (S3 mix with maximum size of particle 19 mm) and Mix-5 (S4 mix with maximum size of particle as 12.5 mm) were compared to quantify the effects of gradation on dynamic modulus. These two mixes were compared because they have similar binder content but different mix gradations. The comparison was made at 6% air voids which represents the typical target compaction of an asphalt pavement. It was observed that larger size of aggregates produces larger dynamic modulus compared to smaller size of particles. Both mixes showed similar dynamic modulus values at lower temperatures, while they differed significantly at higher temperature.

3.6.4 Effect of Binder Types on Dynamic Modulus

Mix-1 and Mix-2 were compared to examine the effects of the binder type on dynamic modulus. These two mixes were compared because both types of has similar aggregate gradation but

different binder types. The comparison was made at 6% air voids. It was observed that Mix-1 with PG 64-22 produced larger dynamic modulus compared to Mix-2 with PG 76-28 binder. It was concluded that a higher percentage of RAP resulted Mix-1 stiffer compared to Mix-2.

4. EVALUATION OF PREDICTIVE MODELS FOR ESTIMATING DYNAMIC MODULUS OF HMA MIXES USED IN OKLAHOMA

As discussed in the previous section, the dynamic modulus of hot mix asphalt (HMA) mixes is an important input parameter for the design of asphalt pavements (Fat et al., 2009; Bari and Witczak, 2006; Obulareddy*, 2002;* Birgisson et al., 2005; Dongre et al., 2005; Tran and Hall, 2005; NCHRP, 2004; Loulizi et al., 2007; Singh et al., 2011)*.*The Mechanistic-Empirical Pavement Design Guide (MEPDG) recommends the use of dynamic modulus at all three levels (i.e., Level 1, Level 2, and Level 3) of analysis for predicting the performance of flexible pavements. The use of a particular hierarchal input level of analysis depends on the amount of information available to the designer and the criticality of the project. For example, at Level 1, the asphalt binder and the HMA mix are tested in the laboratory to measure dynamic modulus. However, the measurement of dynamic modulus in the laboratory is not always feasible, as it is a tedious experiment, and may take several days to develop a single master curve (Obulareddy, 2002; Birgisson et al., 2005; Azari et al., 2007). Moreover, it requires costly equipment and trained personnel for specimen preparation, testing and data analysis (Azari et al., 2007*)*. To overcome these difficulties, the MEPDG recommends the Level 2 and Level 3 designs to estimate dynamic modulus without conducting actual modulus tests in the laboratory. Several predictive models are available in the literature for estimation of dynamic modulus of a HMA mix. These models utilize the volumetric properties of a mix, aggregate gradation, loading frequency, and viscosity of an asphalt binder to predict dynamic modulus (Tran and Hall, 2005; Al-Khateeb et al., 2006; Christensen et al., 2003; Andrei et al., 1999).

In recent years, the Witczak 1999 (Andrei et al., 1999), Witczak 2006 (Bari and Witczak, 2006), Hirsch (Christensen et al., 2003), and Al-Khateeb (Al-Khateeb et al., 2006) models have been increasing used to estimate dynamic modulus of asphalt mixes. While predictive models are convenient, their performance varies with the type of mixes and volumetric properties (Bari and Witczak, 2006; Obulareddy*, 2002;* Birgisson et al., 2005; Dongre et al., 2005; Tran and Hall, 2005; Azari et al., 2007; Kim et al., 2005; Schwartz, 2005; Pellinen and Witczak, 2002). Obulareddy, (2003)*,* Birgisson et al., (2005), Tran (2006), and Kim et al., (2005) evaluated the performance of the Witczak 1999 model for mixes that are commonly used in Louisiana, Florida, Arkansas, and North Carolina, respectively. Their research revealed that the Witczak 1999 model over-predicted dynamic modulus. The performance of this model was also found to be inconsistent across different types of asphalt mixes (Bari and Witczak, 2006; Dongre et al., 2005; Azari et al., 2007; Schwartz, 2005; Pellinen and Witczak, 2002). The revised Witczak

2006 model was introduced to improve the prediction accuracy of the Witczak 1999 model. The revised Witczak 2006 model has been the subject of many recent studies (Fat et al., 2009; Azari et al., 2007; Abdo et al., 2009; Ceylan et al., 2009). It was observed that this model also over-predicts dynamic modulus, and exhibits increased error at extremely high and low temperature conditions. Bari et al., (2006), Obulareddy (2006), Kim et al., (2005), and Ceylan et al., (2008) conducted studies to check the performance of the Hirsch model. It was reported that this model under-predicted dynamic modulus compared to the measured values. The Al-Khateeb model, on the other hand, showed substantial bias at low temperature and a reduced sensitivity at high temperature (Far et al., 2009).

Use of these predictive models in the mechanistic-empirical design of asphalt pavements will be error prone, if the performance of these models is not accounted for in the design process. Therefore, it is important to evaluate the performance of each model for a wide range of asphalt mixes at different air voids and test conditions.

In this section, the performance of four predictive models, namely, Witczak 1999, Witczak 2006, Hirsch, and Al-Khateeb in estimation of dynamic modulus of selected HMA mixes that are commonly used in Oklahoma evaluated. Based on these, calibration factors are developed for each of these models to improve the prediction accuracy for Level 2 and Level 3 designs of the MEPDG.

4.1 DYNAMIC MODULUS PREDICTIVE MODELS

4.1.1 Witczak 1999 Model

Andre et al., (1999) developed the Witczak 1999 model using 2750 test data points from 205 HMA mixes. This model is currently used in the Level 2 and Level 3 designs of the MEDPG. The model is given by Equation (1).

$$\begin{aligned}\text{Log } E^* = {} & -1.249937 + 0.029232\,\rho_{200} - 0.001767\,(\rho_{200})^2 - 0.002841\rho_4 \\ & - 0.058097\,V_a - 0.8022\,\frac{V_{beff}}{(V_{beff} + V_a)} \\ & + \frac{3.87197 - 0.0021\rho_4 + 0.003958\,\rho_{38} - 0.000017(\rho_{38})^2 + 0.00547\,\rho_{34}}{1 + e^{(-0.603313 - 0.31335\log(f) - 0.393532\log(\eta))}}\end{aligned} \quad (4.1)$$

where,

E* = Asphalt mix dynamic modulus (10^5 psi),

η = Viscosity of binder (10^6 poise),

f = Loading frequency (Hz),

V_a = Air voids in the mix (% by volume),

V_{beff} = Effective binder content (% by volume),

ρ_{200} = % Passing # 200 (0.075 mm) sieve,

ρ_4 = Cumulative % retained on # 4 (4.75 mm) sieve,

ρ_{38} = Cumulative % retained on 3/8 inch (9.5 mm) sieve, and

ρ_{34} = Cumulative % retained on 3/4 inch (19 mm) sieve.

4.1.2 Witczak 2006 Model

Bari et al., (2006) revised the Witczak 1999 model, using 7400 data points from 346 HMA mixes. The Witczak 2006 model uses dynamic shear modulus ($|G_b^*|$) and phase angle (δ_b) of binder as input parameters. The revised model can be expressed as:

$$
\begin{aligned}
Log_{10} E^* = {} & -0.349 \\
& + 0.754\,(|G_b^*|^{-0.0052}) \times \begin{pmatrix} 6.65 - 0.032\rho_{200} + 0.0027\,(\rho_{200})^2 + 0.011\,\rho_4 - 0.0001\,\rho_4{}^2 \\ +0.006\,\rho_{38} - 0.00014\,(\rho_{38})^2 - 0.08\,V_a - 1.06\,\dfrac{V_{beff}}{(V_{beff}+V_a)} \end{pmatrix} \\
& + \frac{2.56 + 0.03V_a + 0.71\,\dfrac{V_{beff}}{(V_{beff}+V_a)} + 0.012\,\rho_{38} - 0.0001(\rho_{38})^2 - 0.01\,\rho_{34}}{1 + e^{(-0.7814 - 0.5785\,log(|G_b^*|) + 0.8834\,log(\delta_b))}}
\end{aligned}
\qquad (4.2)
$$

where,

E* = Dynamic modulus (psi),

ρ_{200} , ρ_4 , ρ_{38} , ρ_{34} , V_a, V_{beff} as defined previously in Equation (1),

$|G_b^*|$ = Dynamic shear modulus of asphalt binder (psi), and

δ_b = Phase angle of asphalt binder (degree).

4.1.3 Hirsch Model

Christensen et al., (2003) modified Hirsch model for estimating dynamic modulus of HMA mixes. Their model is given in Equations (4.3) and (4.4).

$$|\mathrm{E}^*|_\mathrm{m} = P_c\left[4{,}200{,}000\left(1-\frac{\mathrm{VMA}}{100}\right)+3\,|\mathrm{G}^*|_\mathrm{b}\left(\frac{(\mathrm{VMA})(\mathrm{VFA})}{10{,}000}\right)\right] + \frac{1-P_c}{\left[\frac{\left(1-\frac{\mathrm{VMA}}{100}\right)}{4{,}200{,}000}+\frac{VMA}{3\,|\mathrm{G}^*|_\mathrm{b}\,(\mathrm{VFA})}\right]} \quad (4.3)$$

$$P_c = \frac{\left(20+\frac{3\,|\mathrm{G}^*|_\mathrm{b}\,(\mathrm{VFA})}{\mathrm{VMA}}\right)^{0.58}}{650+\left(\frac{3\,|\mathrm{G}^*|_\mathrm{b}\,(\mathrm{VFA})}{\mathrm{VMA}}\right)^{0.58}} \quad (4.4)$$

where,

$|\mathrm{E}^*|_\mathrm{m}$ = Absolute value of asphalt mixture dynamic modulus, (psi),

$|\mathrm{G}^*|_\mathrm{b}$ = Absolute value of asphalt binder complex shear modulus (psi),

VMA = Voids in mineral aggregates in compacted mixture (%), and

VFA = Voids filled with asphalt in compacted mixture (%).

4.1.4 Al-Khateeb Model

Al-Khateeb et al., (2006) developed a model based on law of mixtures. The model is shown in Equation (4.5).

$$|\mathrm{E}^*|_\mathrm{m} = 3\left(\frac{100-\mathrm{VMA}}{100}\right)\left\{\frac{\left(90+1.45\frac{|\mathrm{G}^*|_\mathrm{b}}{\mathrm{VMA}}\right)^{0.66}}{1100+\left(0.13\frac{|\mathrm{G}^*|_\mathrm{b}}{\mathrm{VMA}}\right)^{0.66}}\right\}|\mathrm{G}^*|_\mathrm{g} \quad (4.5)$$

where,

$|\mathrm{E}^*|_\mathrm{m}$ = Absolute value of dynamic modulus, (Pa),

VMA = Voids in mineral aggregate in compacted mixture (%),

$|\mathrm{G}^*|_\mathrm{b}$ = Complex shear modulus of asphalt binder (Pa), and

$|\mathrm{G}^*|_\mathrm{g}$ = Complex shear modulus of asphalt binder in glassy state (Pa).

4.2 MATERIAL AND SAMPLE PREPARATION

A total of five different loose HMA mixes (henceforth referred to as Mix-1, Mix-2, Mix-3, Mix-4, and Mix-5) were collected from the production plant. Three of these are surface mixes with a nominal maximum aggregate size (NMAS) of 12.5 mm, and two are base mixes with a NMAS of 19 mm. The mixes contained three types of aggregates: limestone, granite, and rhyolite, and three different types of performance grade (PG) asphalt binders: PG 64-22, PG 70-28, and PG 76-28. These mixes are commonly used in the construction of asphalt pavements in Oklahoma.

Table 4.1 Mix Gradation and Volumetric Properties

Gradation		**Mix Type**				
(%Passing)		Mix-1	Mix-2	Mix-3	Mix-4	Mix-5
Sieve size (mm)						
25		100	100			
19		98	98	100	100	100
12.5		87	87	97	98	98
9.5		80	80	89	87	87
4.75		58	62	69	62	62
2.36		37	40	49	40	40
1.18		25	27	35	28	28
0.6		19	20	25	21	21
0.3		12	12	15	13	13
0.15		4	5	7	5	5
0.075		2.9	2.8	2.5	3.2	3.2
Volumetric Properties and Test Conditions						
G_{mm}		2.505	2.523	2.463	2.477	2.508
G_{se}		2.671	2.677	2.658	2.681	2.688
G_{sb}		2.645	2.657	2.634	2.669	2.652
G_b		1.01	1.01	1.01	1.02	1.01
Binder Type		PG 64-22	PG 76-28	PG 70-28	PG 64-22	PG 76-28
P_b (%)		4.1	4.1	4.5	5.1	4.2
VMA (%)	Min.	14.11	14.81	16.23	16.6	14.95
	Max.	20.42	20.11	21.55	22.12	20.59
VFA (%)	Min.	39.88	42.86	41.37	47.71	39.24
	Max.	62.21	62.04	58.77	68.09	57.87
Va (%)				6, 8, 10, 12		
T (C)				4, 21, 40, 55		
Frequency (Hz)				25, 10, 5, 1, 0.5, 0.1		
Aggregate Type		Limestone	Limestone	Granite	Rhyolite	Limestone
Mix Type		Recycled	Recycled	Virgin	Virgin	Recycled

G_{mm} = Max. Theoretical Sp. Gr. Mix
G_{se} = Effective Sp. Gr. of Agg.
G_{sb} = Bulk Sp. Gr.of Agg.
G_b = Specific Gravity of Binder
V_a = Air Voids
VMA = Voids in Mineral Agg.
VFA = Voids Filled with Asphalt
T (C) = Temperature
P_b = Binder Content

Each mix was preheated in an oven, and samples were compacted using a Superpave Gyratory Compactor (SGC) at four levels of air voids: 6%, 8%, 10%, and 12%. Three identical specimens were compacted at each air void level. A total of 60 samples were compacted (3 samples each of 5 mixes at 4 different air voids). The gradation and volumetric properties of the mixes used in the tests are given in Table 4.1.

4.3 DYNAMIC MODULUS TESTING

Dynamic modulus tests were performed in accordance with the AASHTO TP62-03 (AASHTO, 2006). All tests were performed using a material testing system (MTS) machine equipped with a servo-hydraulic testing system. The compacted specimens were placed in an environmental chamber, and they were allowed to reach equilibrium for a specified test temperature. Dynamic modulus of each specimen was measured at four different temperatures: 4, 21, 40, and 55^{o}C, and at six different frequencies: 25, 10, 5, 1, 0.5, and 0.1 Hz. Thus, a total of 1440 dynamic modulus values (5 mixes x 4 air voids x 3 samples x 4 temperatures x 6 frequencies) were measured in the laboratory.

4.4 ESTIMATION OF DYNAMIC MODULUS

The Witczak 1999, Witczak 2006, Hirsch, and Al-Khateeb models (Equation (4.1) through Equation (4.5)) were used for estimating dynamic modulus of all the five mixes. The viscosity of each asphalt binder used for the Witczak 1999 model was calculated using the viscosity–temperature relationship (ASTM, 2009) shown in Equation (4.6).

$$\log\log(\eta) = A + VTS\log T_R \quad (4.6)$$

where,

η = Viscosity of binder (cP),

T_R = Temperature (Rankine),

A = Regression intercept, and

VTS = Regression slope of viscosity temperature graph.

The regression parameters in the above equation, namely, the intercept (A) and the slope (VTS), pertaining to the temperature-viscosity relationship for three asphalt binders (i.e., PG 64-22, PG 70-28, and PG 76-28) were taken from the MEPDG guide (NCHRP, 2004). The $|G^*|_b$ and δ required for the Witczak 2006, Hirsch, and Al-Khateeb models were calculated using the model developed by Bari and Witczak,(2007). A total of 1440 dynamic modulus values were estimated using each predictive model.

4.5 EVALUATION OF THE PERFORMANCE OF THE PREDICTIVE MODELS

The performance of each predictive model was evaluated using three different criteria: goodness-of-fit statistics, comparison of the measured and the predicted values with the line of equality (LOE), and the use of local bias statistics (slope, intercept, and average error).

The goodness-of-fit statistics includes the ratio of the standard error of estimate (S_e) to the standard deviation (S_y), and the coefficient of determination (R^2). S_e, S_y, and R^2 for each of the models were calculated according to Equations (4.7) - (4.9). In the analysis of the data, S_e represents the likely error in the prediction. The ratio S_e/S_y can, therefore, be used to assess the accuracy of the predictive model. While S_e/S_y is a measure of the accuracy of the estimates, R^2 represents the accuracy of the model. Together, these two measures can be used to standardize the results in a "subjective goodness" classification (Witczak et al., 2002). The criteria used in the classification are shown in Table 4.2.

$$S_e = \sqrt{\frac{\sum(y-\hat{y})^2}{(n-k)}} \tag{4.7}$$

$$S_y = \sqrt{\frac{\sum(y-\overline{y})^2}{(n-1)}} \tag{4.8}$$

$$R^2 = 1 - \frac{(n-k)}{(n-1)}\left(\frac{S_e}{S_y}\right)^2 \tag{4.9}$$

where,

S_e = Standard error of estimate,

S_y = Standard deviation,

R^2 = Correlation coefficient,

y = Measured dynamic modulus,

$\hat{y}$ = Predicted dynamic modulus,

$\overline{y}$ = Mean value of measured dynamic modulus,

n = Sample size, and

k = Number of independent variables in the model.

The measured and the predicted dynamic modulus values were also compared by plotting them on the LOE plot. If the matching points are clustered along the LOE line, then this would

indicate that the predictive model has a good correlation to the measured data. It is to be noted that the goodness-of-fit statistics and matching the predicted and the measured dynamic modulus values on the LOE line do not conclusively address the model accuracy (Ceylan et al., 2009). Under certain conditions, systemic or local bias in the models can cause significant reduction in the accuracy of the predicted modulus. Therefore, the local bias statistics (slope, intercept) and the average error for each of the predictive models were used to determine the existence of bias. The intercept and slope were calculated by fitting an unconstrained linear trend line that does not pass through the origin (Ceylan et al., 2009). A non-zero slope and average error indicate a consistent over-prediction or under-prediction by the model (Obulareddy, 2006; Tran and Hall, 2005, Ceylan et al., 2009).

Table 4.2 Criteria for Subjective Classification of Goodness-of-fit

Criteria	R^2	S_e/S_y
Excellent	> 0.90	< 0.35
Good	0.70 - 0.89	0.36 - 0.55
Fair	0.40 - 0.69	0.56 - 0.75
Poor	0.20 - 0.39	0.76 - 0.90
Very Poor	< 0.19	> 0.90

4.6 RESULTS AND OBSERVATIONS

4.6.1 Overall Performance Evaluation

4.6.1.1 Goodness-of-Fit Criterion

To assess the overall performance of these models (i.e., Witczak 1999, Witczak 2006, Hirsch, and Al-Khateeb), the goodness-of-fit statistics (S_e/S_y, R^2) were calculated for a combined dataset of the five mixes used in the present study. A total of 1440 laboratory measured dynamic modulus values were used to check the strengths and weaknesses of each model. The S_e/S_y and R^2 values were calculated at logarithmic and arithmetic scales using Equation (4.7) through Equation (4.9).

Table 4.3 summarizes the goodness-of-fit statistics calculated at logarithmic and arithmetic scales. It can be seen that the performance of the Witczak 1999 and Hirsch models was rated as 'good' both in the logarithmic and the arithmetic scales (Figure 4.1(a), Table 4.3). These results are consistent with those reported by Bari et al., (2006) and Tran et al., (2005). In comparison, the performance of both the Witczak 2006 and the Al Khateeb models were seen to be inferior to the performance of the Witczak 1999 and Hirsch models.

4.6.1.2 LOE Criterion

The predicted and the measured dynamic modulus values were plotted on the LOE plot. Figure 4.2(a) shows that the predictions obtained using the Witczak 1999 model are tightly clustered around the LOE. This indicates that dynamic modulus values predicted by the Witczak 1999 model are in 'good' match with the measured dynamic modulus. The modulus values predicted by the Witczak 2006 model match well at values corresponding to low stiffness; however, there is a significant mismatch between the measured and the predicted values at higher stiffness (Figure 4.2 (b)). Similarly, the modulus values predicted by the Hirsch model are dispersed around the LOE line, indicating this model exhibits significant error (Figure 4.2 (c)). The Al-Khateeb model exhibits large deviations at low stiffness, indicating that this model is not sensitive at low values of modulus (Figure 4.2 (d)).

Table 4.3 Overall Performance Evaluation on Combined Dataset: Goodness-of-fit Statistics

Model	Logarithmic Scale			Arithmetic Scale		
	S_e/S_y	R^2	Rating	S_e/S_y	R^2	Rating
Witczak 1999	0.39	0.85	Good	0.53	0.72	Good
Witczak 2006	0.62	0.61	Fair	1.57	< 0.19	Very Poor
Hirsch	0.52	0.73	Good	0.41	0.83	Good
Al-Khateeb	0.82	0.33	Poor	0.51	0.74	Good

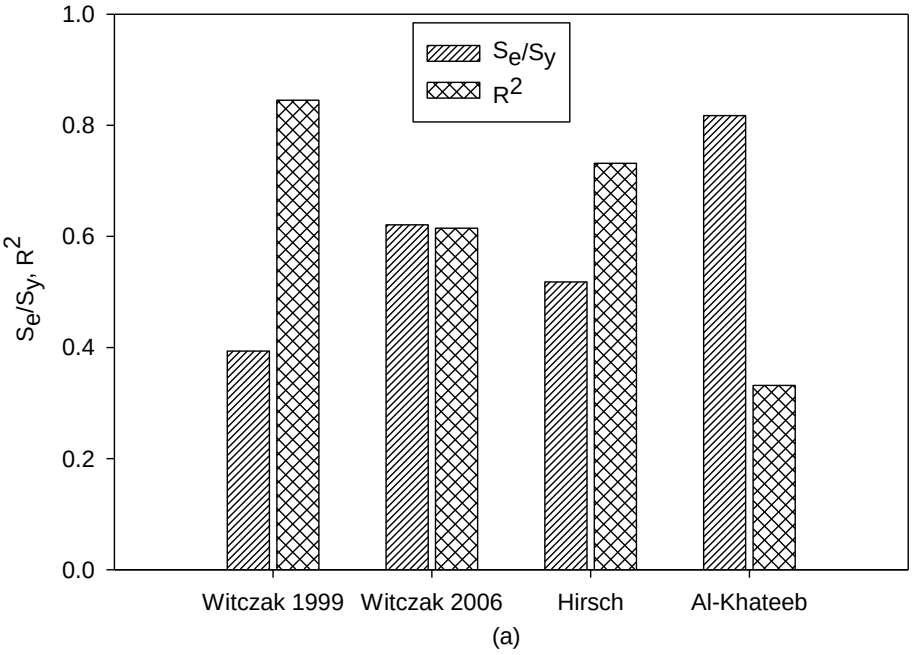

(a)

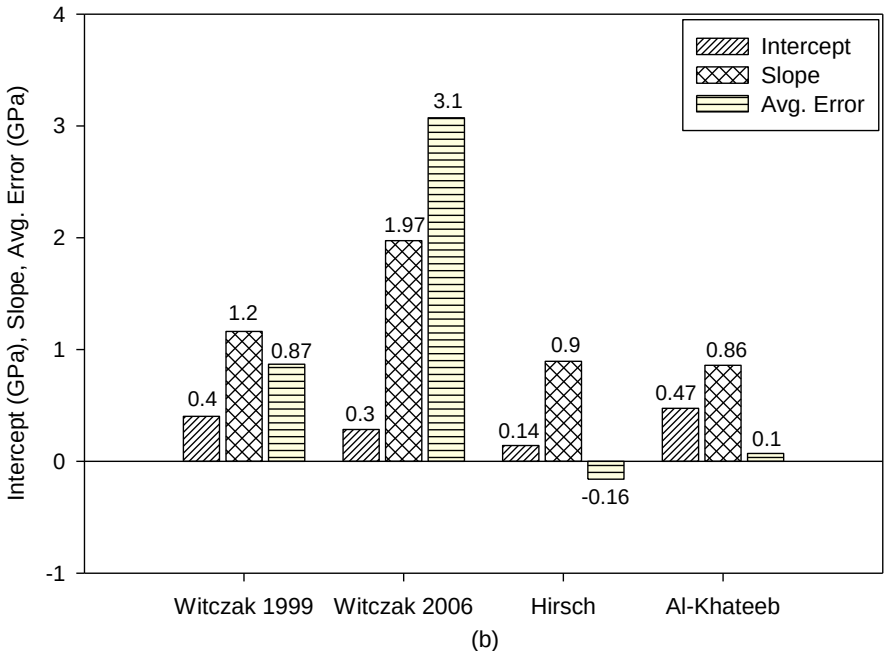

(b)

Figure 4.1 Overall Performance Evaluation (a) S_e/S_y, R^2 (b) Intercept, Slope, and Average Error

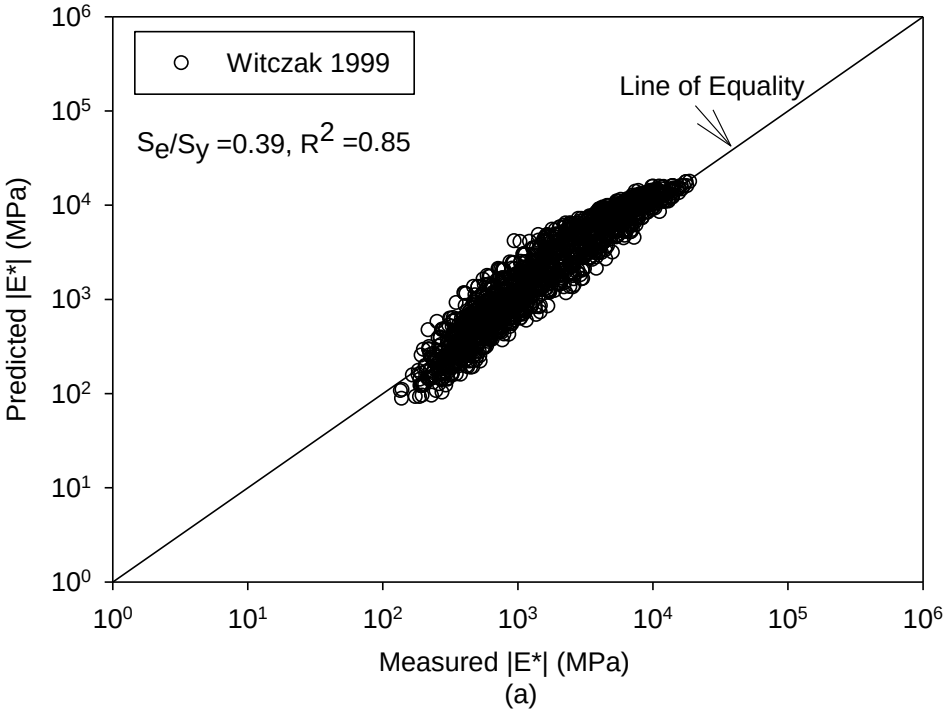
Witczak 1999
Line of Equality
S_e/S_y =0.39, R^2 =0.85
Predicted |E*| (MPa)
Measured |E*| (MPa)
10^0
10^1
10^2
10^3
10^4
10^5
10^6

(a)

f

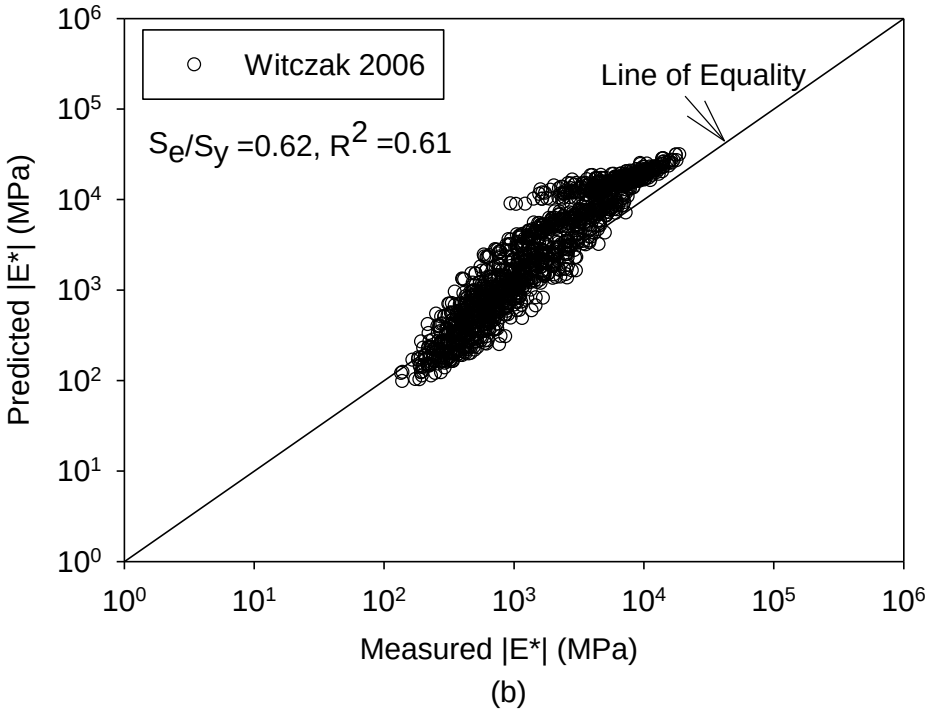
Witczak 2006
Line of Equality
S_e/S_y =0.62, R^2 =0.61
Predicted |E*| (MPa)
Measured |E*| (MPa)
10^0
10^1
10^2
10^3
10^4
10^5
10^6

(b)

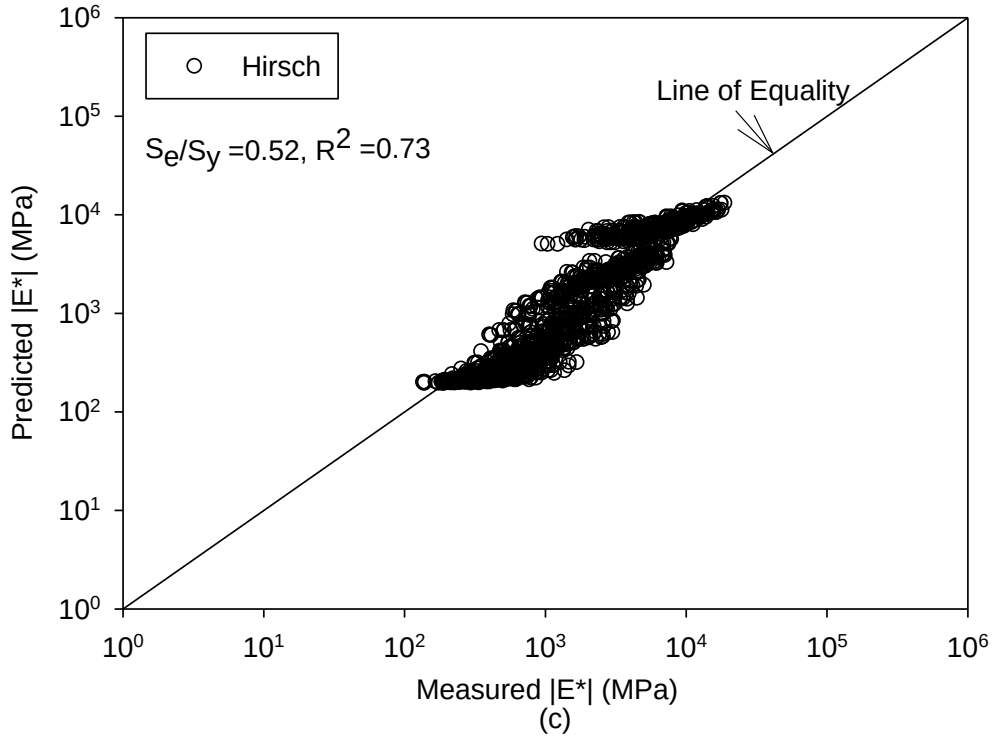

(c)

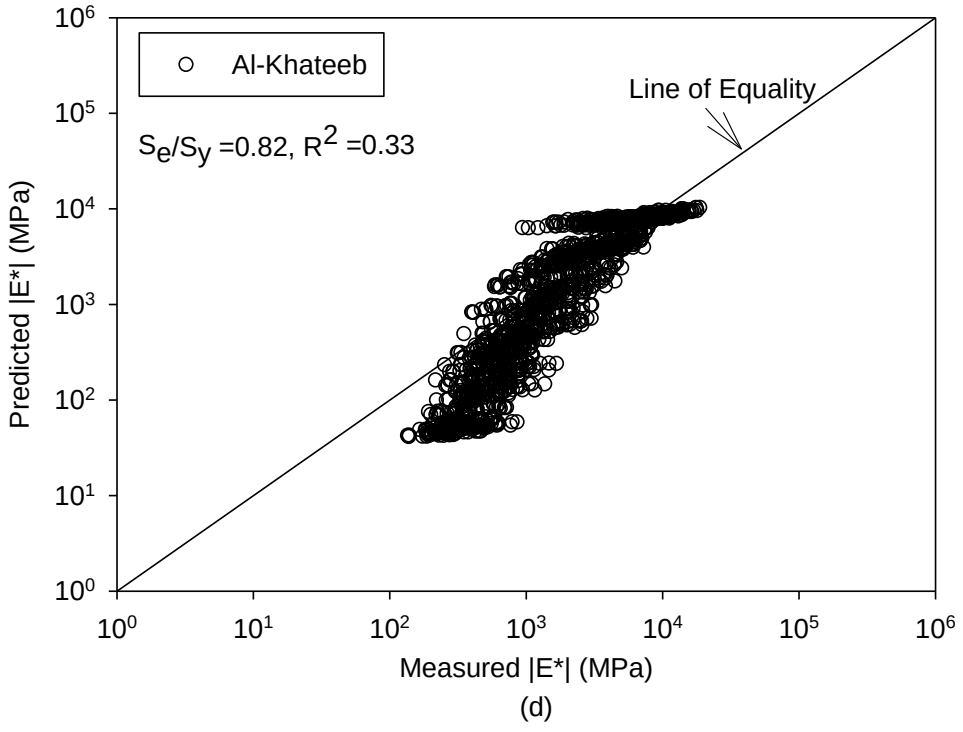

(d)

Figure 4.2 LOE Plots for Overall Performance (a) The Witczak 1999, (b) The Witczak 2006, (c) The Hirsch, and (d) The Al-Khateeb Models

4.6.1.3 Local Bias Statistics Criterion

The relationship between the predicted and the measured values was investigated to determine the intercept, slope, and average error for each of the four models (Figure 4.1 (b)). The Witczak 1999 model shows a low intercept (0.40 GPa) and a slope close to 1 (1.2). The average error for this model was calculated as 0.87 GPa, indicating that it over-estimates dynamic modulus. Similar observations were also reported by other researchers (Obulareddy, 2006; Tran and Hall, 2005; Abdo et al., 2009). The Witczak 2006 model demonstrated the highest average error (3.1 GPa) and maximum slope (1.97 GPa) in comparison with the corresponding values for the other models. Thus, this model over-estimates dynamic modulus of the mix significantly. The Hirsch model exhibits the lowest intercept (0.14 GPa) and the lowest average error (-0.16 GPa), indicating that a low bias exists for this model. The Al-Khateeb model shows the highest intercept (0.47 GPa), indicating that a significant bias exists in this model.

Based on the discussion above, it can be concluded that the performance of the Witczak 1999, and the Hirsch model is ‘good’, while the Witczak 2006 and the Al-Khateeb model produce relatively ‘poor’ estimates of dynamic modulus.

4.6.2 Performance Evaluation at Individual Level of Air Voids

4.6.2.1 Goodness-of-Fit Criterion

Strengths and weaknesses of each predictive model were checked at four levels of air voids (i.e., 6%, 8%, 10%, and 12%). The Witczak 1999 model shows an 'excellent' goodness-of-fit statistics at 6% air voids (Figure 4.3, Table 4.4). In addition, the performance of this model was rated 'good' at three other levels of air voids (i.e., 8%, 10%, and 12%) (Table 4.4). It is important to note that with increasing air voids (i.e., 6% to 12%), S_e/S_y ratio increases and R^2 value decreases, indicating that the model results in significant errors at higher air voids.

The performance of the Witczak 2006 model deteriorates rapidly with increasing air voids. The performance of the model is 'good' at 6% air voids, while the accuracy deteriorates at higher levels of air voids (Figure 4.3, Table 4.4). The Hirsch model was rated 'fair' at 6% air voids, and it was rated 'good' at higher air voids (Figure 4.3, Table 4.4). The performance of the Al-Khateeb model was found to be 'poor' at all four levels of air voids (Figure 4.3, Table 4.4).

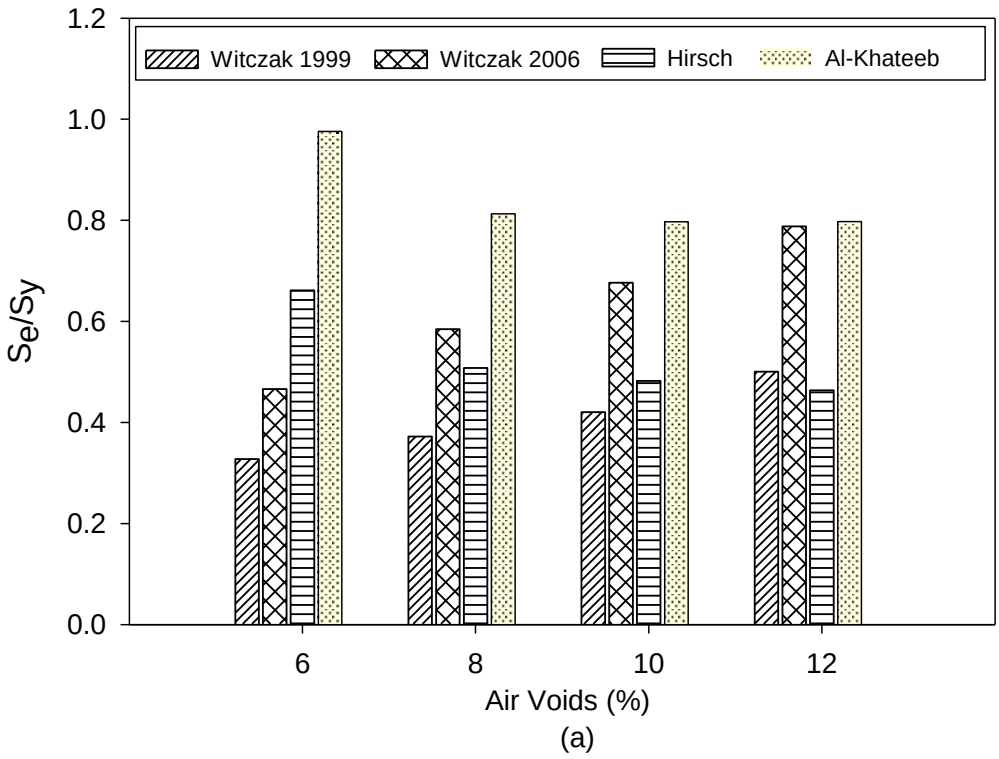

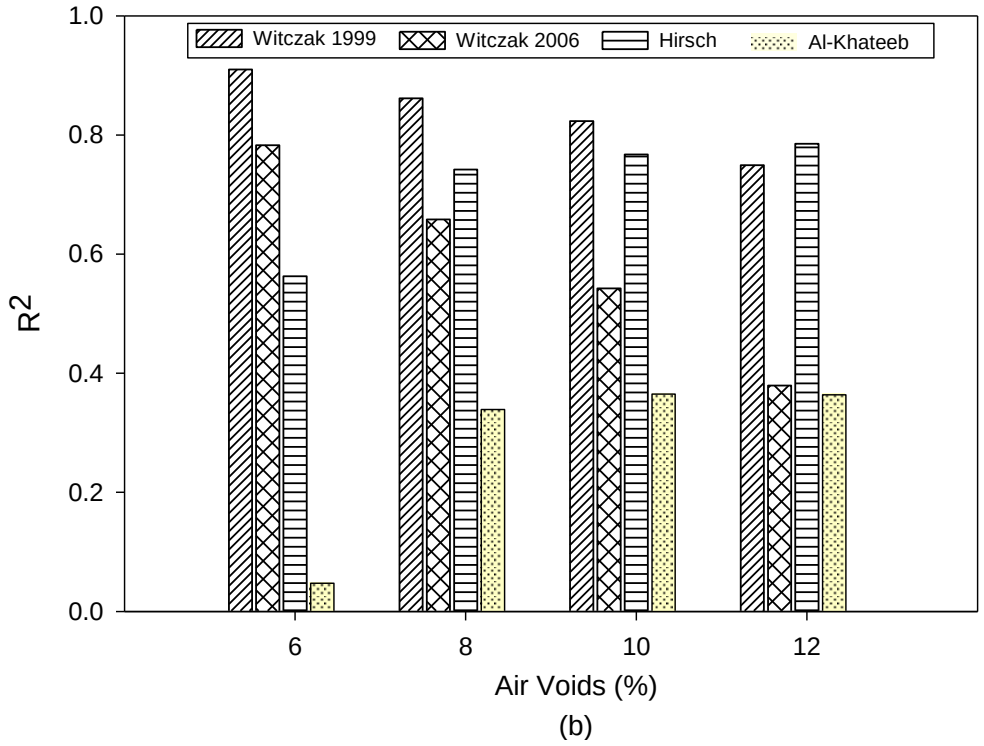

Figure 4.3 Goodness-of-Fit Statistics at Each Level of Air Voids (a) S_e/S_y (b) R^2

Table 4.4 Goodness-of-Fit Statistics at Individual Level of Air Voids

Witczak 1999						
Air Voids	Logarithmic Scale			Arithmetic Scale		
(%)	S_e/S_y	R^2	Rating	S_e/S_y	R^2	Rating
6	0.33	0.91	Excellent	0.31	0.91	Excellent
8	0.37	0.86	Good	0.52	0.73	Good
10	0.4	0.82	Good	0.74	0.46	Fair
12	0.5	0.75	Good	0.89	0.20	Poor

Witczak 2006						
Air Voids	Logarithmic Scale			Arithmetic Scale		
(%)	S_e/S_y	R^2	Rating	S_e/S_y	R^2	Rating
6	0.47	0.78	Fair/Good	1.16	<0.19	Very Poor
8	0.58	0.66	Fair	1.51	<0.19	Very Poor
10	0.7	0.54	Fair	2.02	<0.19	Very Poor
12	0.8	0.38	Poor	2.45	<0.19	Very Poor

Hirsch						
Air Voids	Logarithmic Scale			Arithmetic Scale		
(%)	S_e/S_y	R^2	Rating	S_e/S_y	R^2	Rating
6	0.66	0.56	Fair	0.39	0.85	Good
8	0.51	0.74	Good	0.37	0.86	Good
10	0.5	0.77	Good	0.45	0.80	Good
12	0.5	0.79	Good	0.63	0.60	Fair

Al-Khateeb						
Air Voids	Logarithmic Scale			Arithmetic Scale		
(%)	S_e/S_y	R^2	Rating	S_e/S_y	R^2	Rating
6	0.98	0.05	Very Poor	0.45	0.80	Good
8	0.81	0.34	Poor	0.43	0.82	Good
10	0.8	0.36	Poor	0.56	0.68	Fair
12	0.8	0.36	Poor	0.90	0.19	Very Poor

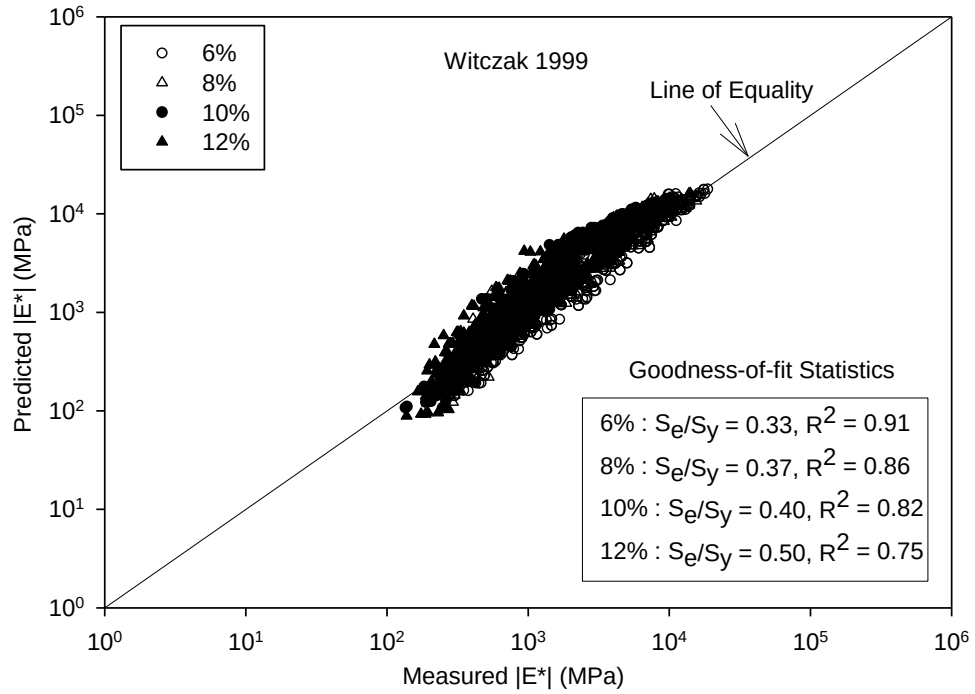
6%
8%
10%
12%
Witczak 1999
Line of Equality
Goodness-of-fit Statistics
6% : Se/Sy = 0.33, R2 = 0.91
8% : Se/Sy = 0.37, R2 = 0.86
10% : Se/Sy = 0.40, R2 = 0.82
12% : Se/Sy = 0.50, R2 = 0.75
Predicted |E*| (MPa)
Measured |E*| (MPa)
10^0
10^1
10^2
10^3
10^4
10^5
10^6

(a)

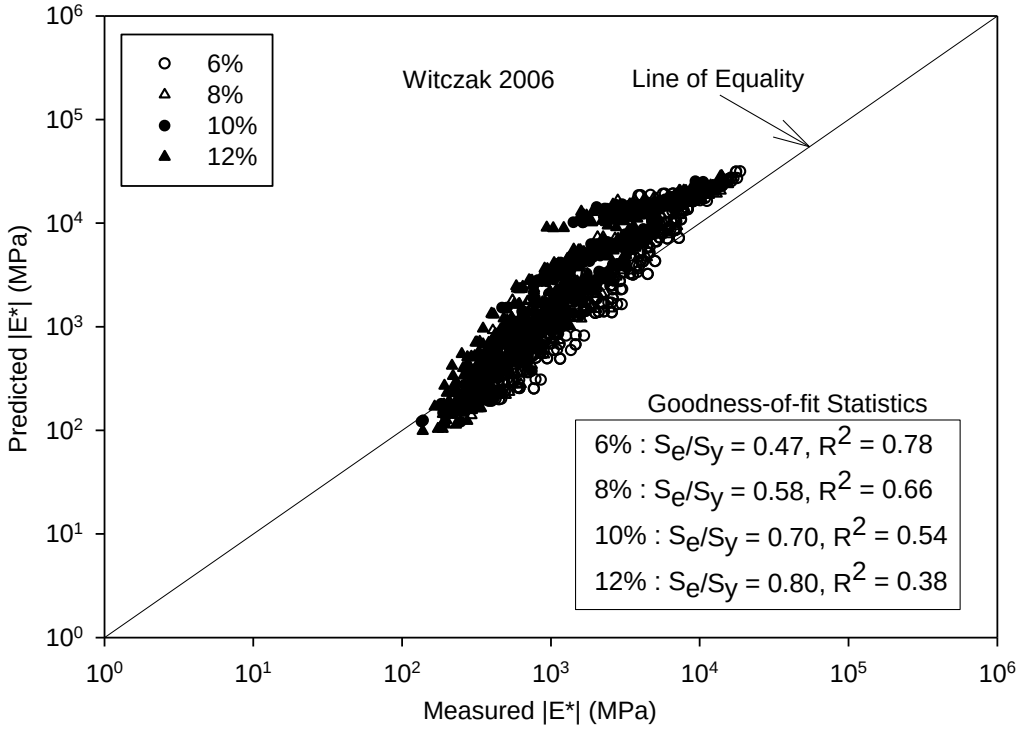
6%
8%
10%
12%
Witczak 2006
Line of Equality
Goodness-of-fit Statistics
6% : Se/Sy = 0.47, R2 = 0.78
8% : Se/Sy = 0.58, R2 = 0.66
10% : Se/Sy = 0.70, R2 = 0.54
12% : Se/Sy = 0.80, R2 = 0.38
Predicted |E*| (MPa)
Measured |E*| (MPa)
10^0
10^1
10^2
10^3
10^4
10^5
10^6

(b)

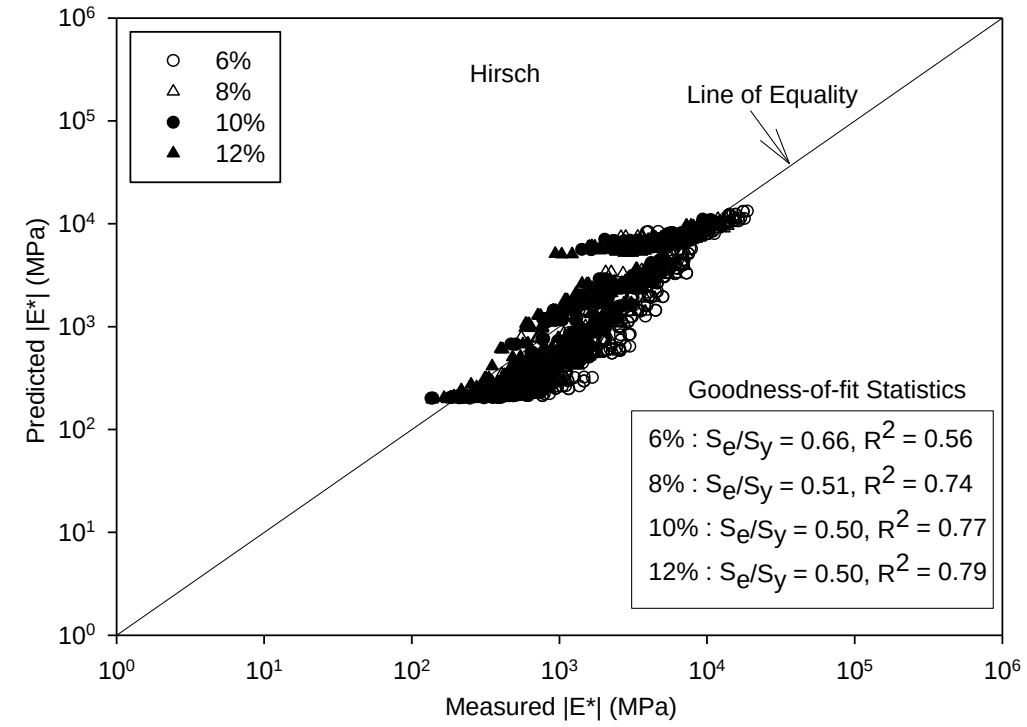

(c)

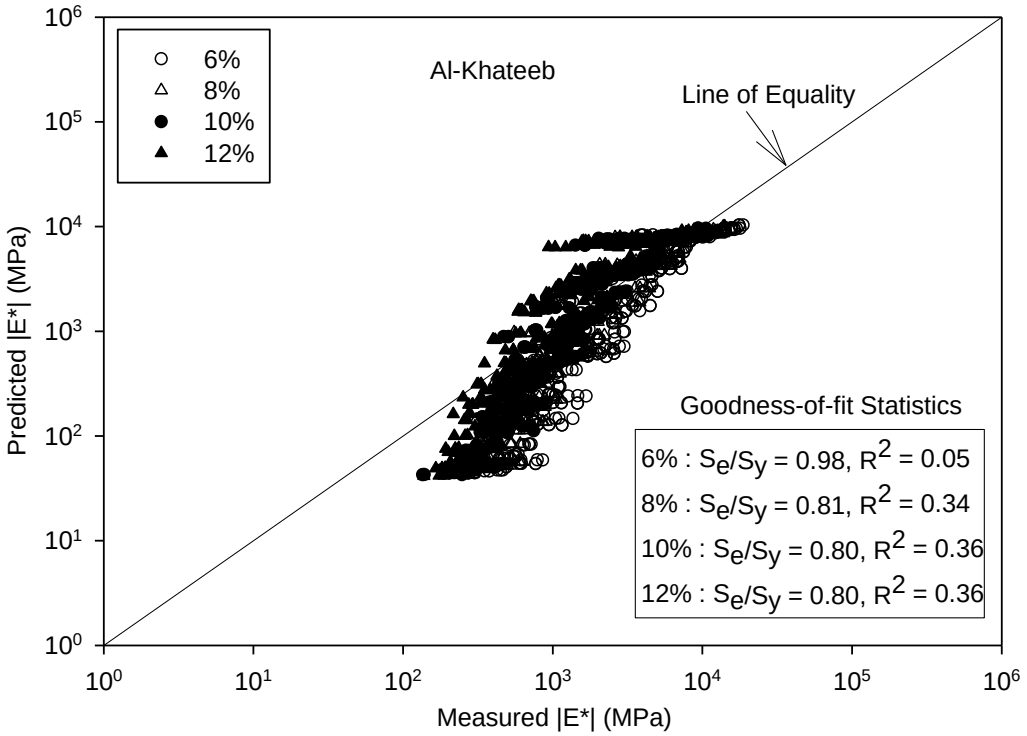

(d)

Figure 4.4 LOE Plot at Each Level of Air Voids (a) The Witczak 1999, (b) The Witczak 2006, (c) The Hirsch, and (d) The Al-Khateeb models

4.6.2.3 Local Bias Statistics Criterion

The slope, intercept, and average error for all the models calculated at four different levels of air voids are presented in Figure 4.5.

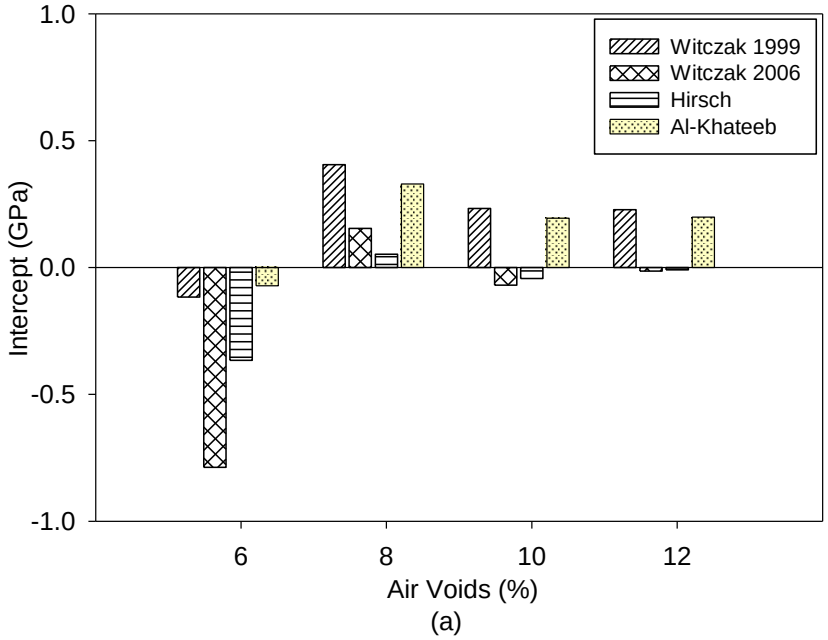

(a)

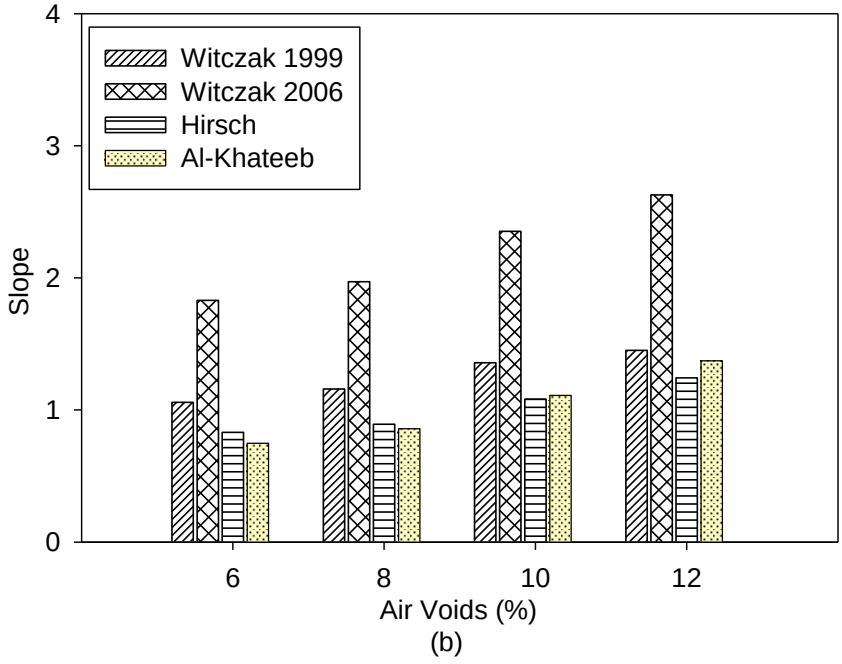

(b)

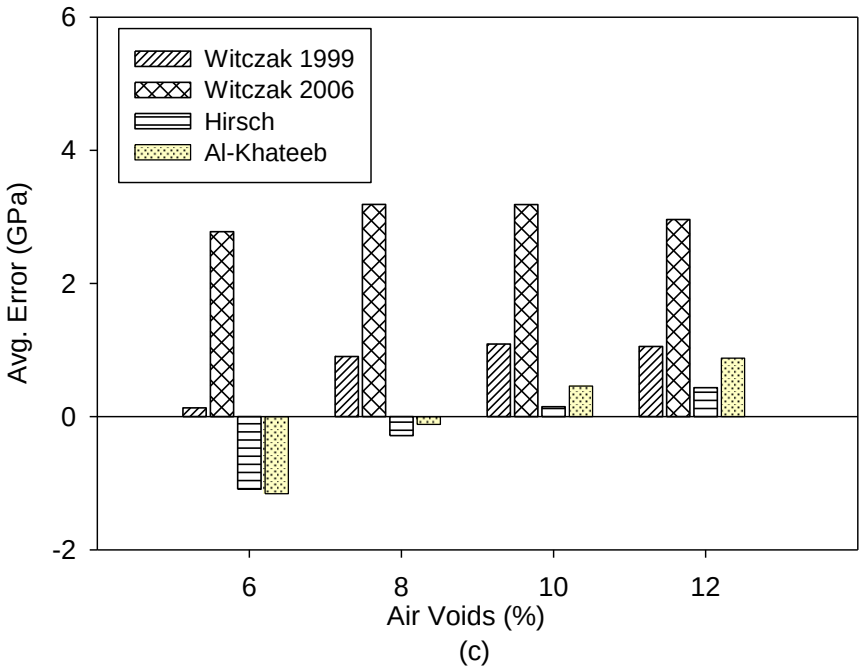

Figure 4.5 Local Bias Statistics at Each Level of Air Voids (a) Intercept, (b) Slope, and (c) Average Error

The intercept for the Witczak 1999 model was observed to be less than 0.5 GPa. The slope increases with increasing air voids, indicating that this model over-predicts dynamic modulus at higher air voids. Similarly, the Witczak 2006 model yields the highest slope, indicating over-estimation of modulus. The slope calculated for the Hirsch and the Al-Khateeb models was observed close to 1. The average error was found to be maximum for the Witczak 2006 model, while it was less than 1 GPa for other models.

It can be concluded that the performance of the Witczak 1999 model can be rated as 'excellent' at lower levels of air voids. However, the accuracy of the predicted dynamic modulus values reduces as the air voids increase. The performance of the Hirsch model is rated 'good' at higher levels of air voids. The Witczak 2006 and the Al-Khateeb models perform poorly at all levels of air voids.

4.6.3 Performance Evaluation with Temperature

The performance of each predictive model was evaluated at four temperatures: 4, 21, 40, and 55^{o}C. Figure 4.6 presents the plot of average error calculated for different levels of air voids, and temperatures. The negative and positive errors indicate under-prediction and over-prediction, respectively.

At 4^{o}C, the Hirsch and the Al-Khateeb models show the lowest average error for all levels of compaction (Figure 4.6 (a)). The Witczak 2006 model, on the other hand, had the largest error for all levels of compaction. The Witczak 1999 model performed well at lower air voids, however, it over-predicts dynamic modulus at higher air voids (Figure 4.6 (a)). These findings are consistent with the results reported in the literature (Far et al., 2009; Birgisson et al., 2005; Dongre et al., 2005; Ceylan et al., 2008, 2009).

The accuracy of the Hirsch and the Al-Khateeb models is poor at 21^{o}C. The Hirsch model under-predicts dynamic modulus for all levels of air voids, while, the Al-Khateeb model over-predicts the modulus at higher air voids. The Witczak 1999 model shows excellent accuracy at 6% air voids, however, it shows poor accuracy at higher air voids. Both the Witczak 1999 and the Witczak 2006 models over-estimate dynamic modulus at higher air voids (Figure 4.6 (b)).

The Witczak 1999 and the Witczak 2006 models show small average errors (< 0.30 GPa) at high temperatures (40^{o}C, 55^{o}C) for all levels of air voids. At higher test temperatures (40^{o}C, 55^{o}C), both the Hirsch and the Al-Khateeb models under-predict dynamic modulus for all levels of air voids (Figure 4.6 (c), (d)).

It can be concluded that the Witczak 1999 model performs reasonably well at intermediate and high temperatures, however, it over-estimates modulus at lower temperatures. The Witczak 2006 model over-predicts dynamic modulus at low and intermediate temperatures, while its performance is excellent at high temperatures. The Hirsch and the Al-Khateeb models under-predict dynamic modulus at higher temperatures.

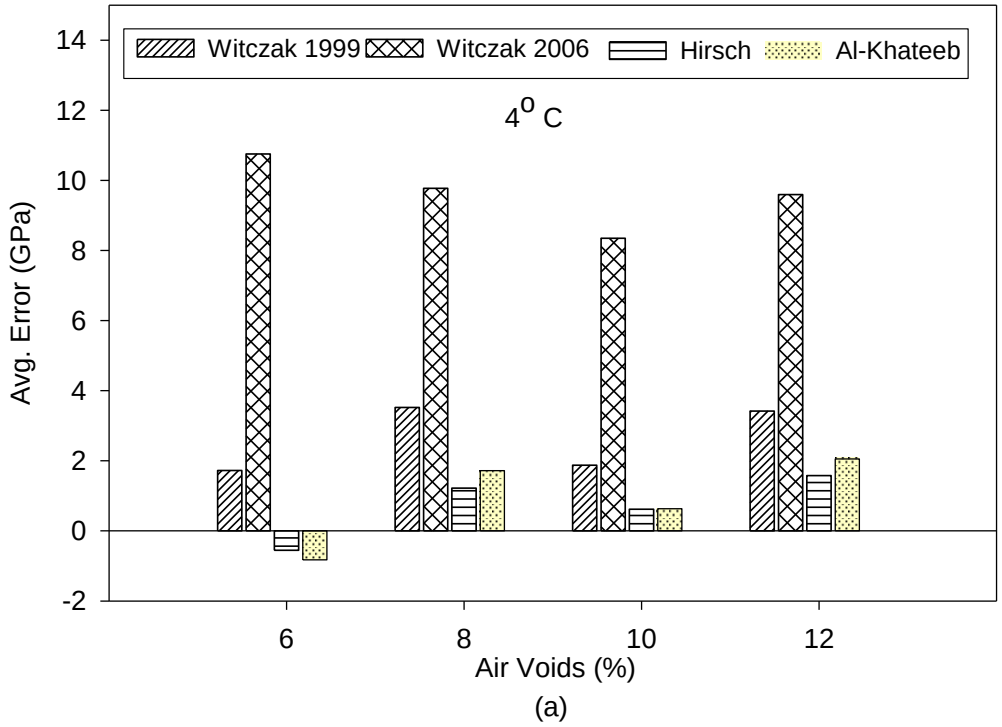
Witczak 1999
Witczak 2006
Hirsch
Al-Khateeb
4° C
Avg. Error (GPa)
14
12
10
8
6
4
2
0
-2
6
8
10
12
Air Voids (%)

(a)

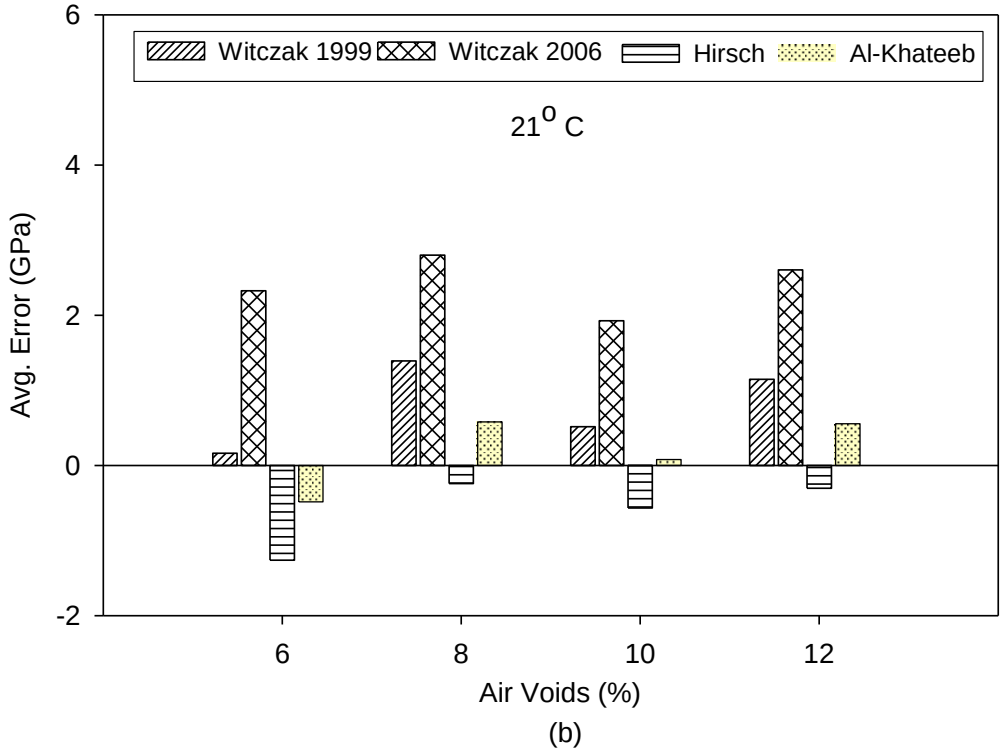
Witczak 1999
Witczak 2006
Hirsch
Al-Khateeb
21° C
Avg. Error (GPa)
6
4
2
0
-2
6
8
10
12
Air Voids (%)

(b)

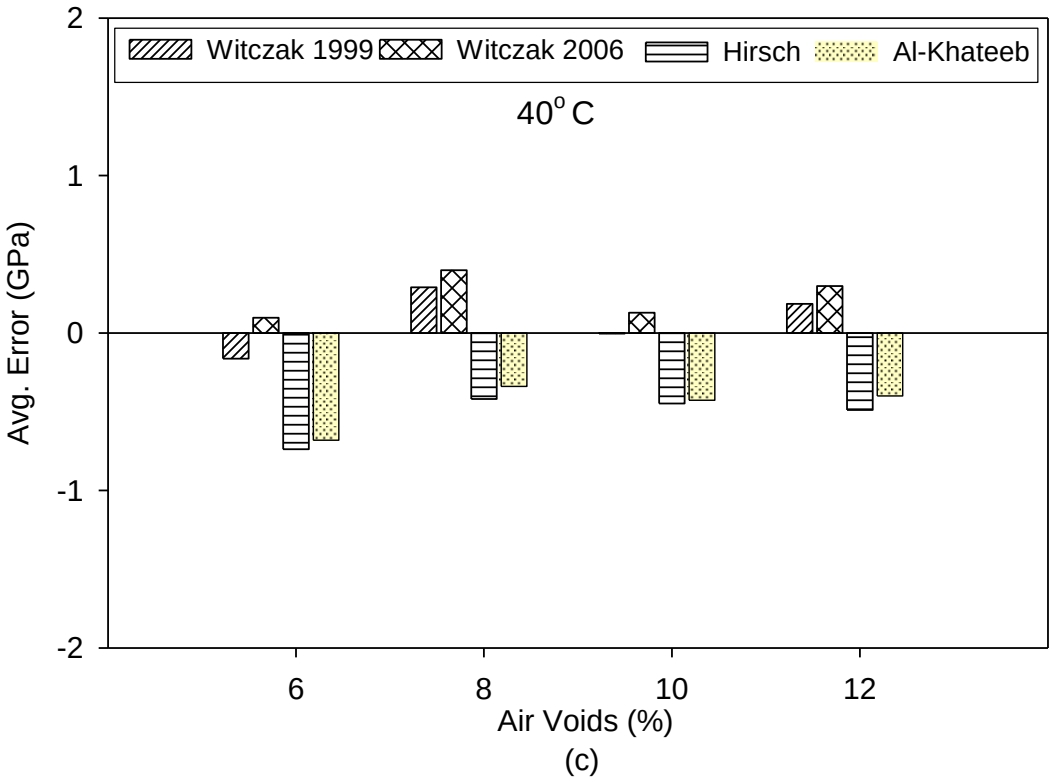

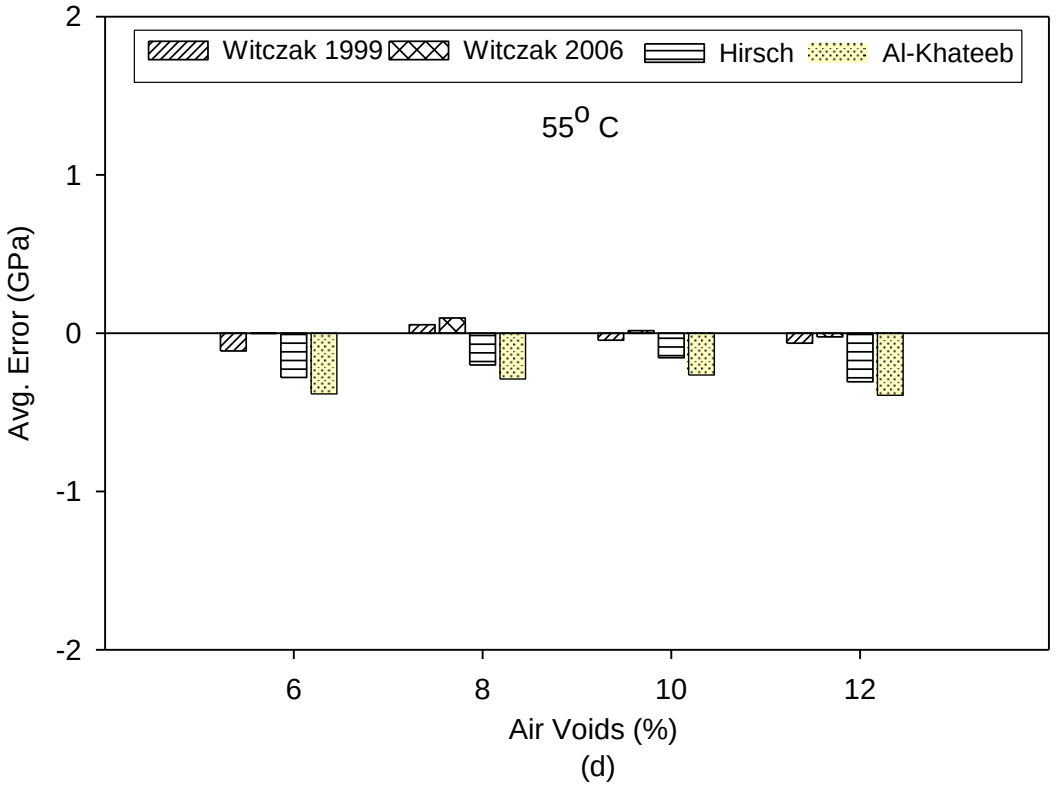

Figure 4.6 Average Error with Temperature at Each Level of Air Voids (a) 4°C, (b) 21°C, (c) 40°C, and (d) 55°C

4.6.4 Development of Calibration Factors

From the discussion in the previous section, dynamic modulus estimated by the Witczak 1999, Witczak 2006, Hirsch, and Al-Khateeb models depends on the temperature, as well as the level of compaction of a specimen. This error has to be corrected before the model can be used in Level 2 and Level 3 designs of the MEPDG. In this study, a linear regression model is used to determine the calibration factor, i.e. the slope, required for such a correction. It can be seen from Figure 4.7(a) that the slope (correction factor) of the linear regression line decreases with increasing air voids for each of the prediction models considered in this study. Therefore, the accuracy of the estimated modulus can be improved by considering the calibration factor at the corresponding air voids rather than using the average calibration factor determined across all the air voids. Failure to account for the variation in the estimated modulus due to air voids can result in significant errors. Figure 4.7 (b) shows the percent error in the predicted modulus when an average calibration factor is used instead of a calibration factor determined at the appropriate air voids. This error in estimation of dynamic modulus might impact the performance of flexible pavements (i.e., rutting, fatigue cracking, and thermal cracking). The relationship between the air voids and the calibration factor for all four predictive models is shown in Figure 4.7 (c).

It is anticipated that use of calibration factors would be helpful in estimating dynamic modulus without conducting actual modulus tests. Moreover, calibration factors are important for the Level 2 and Level 3 designs of the MEPDG.

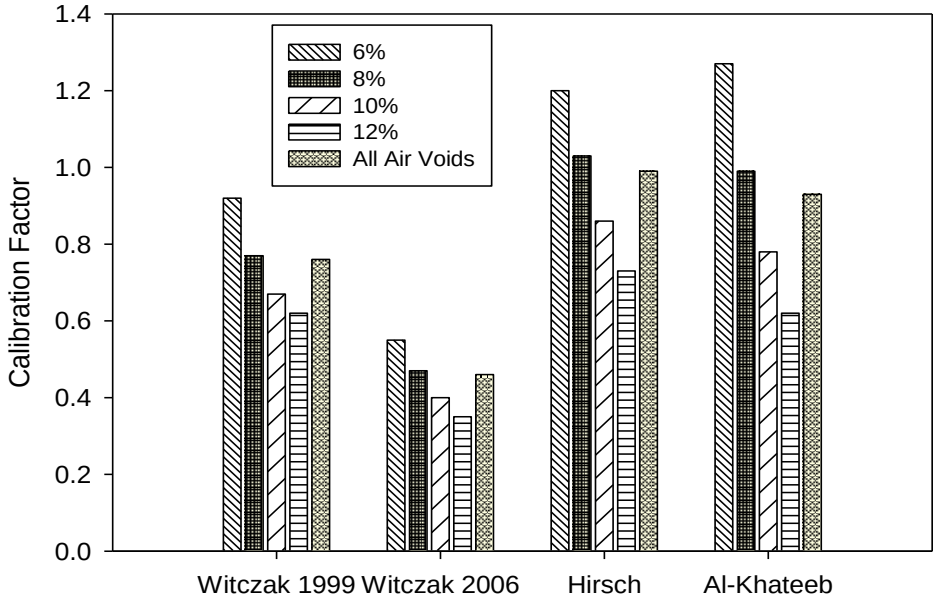

(a)

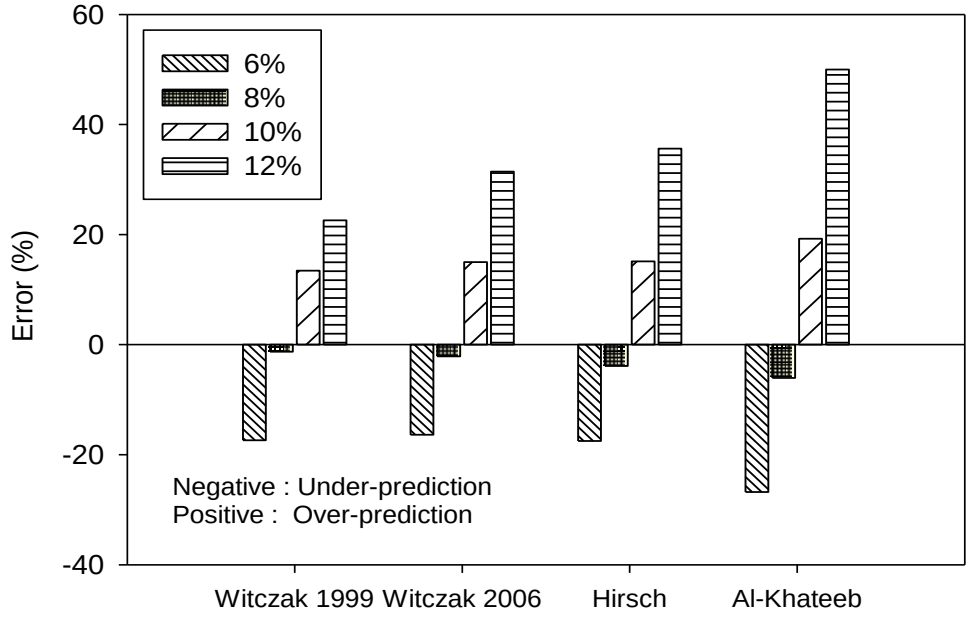

(b)

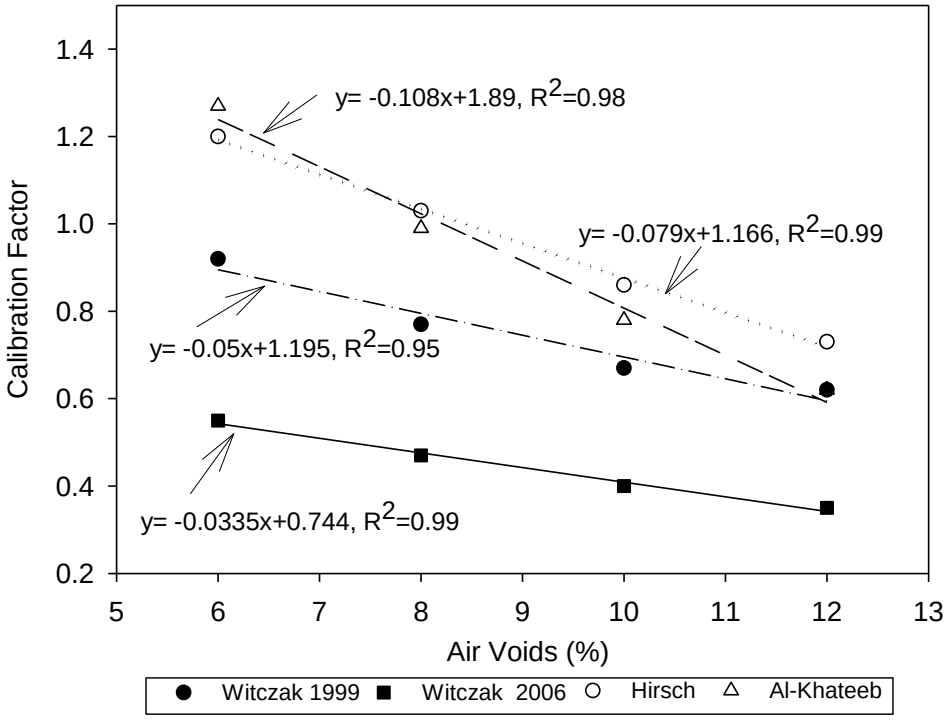

(c)

Figure 4.7 (a) Calibration Factor at Each Level of air Voids, (b) Estimated Error Associated with Calibration Factor, and (c) Relationship between the Calibration Factors and Air Voids

4.7 OBSERVATIONS FROM THE STUDY

In this section, the performance of four predictive models (i.e., Witczak 1999, Witczak 2006, Hirsch, and Al-Khateeb) was evaluated for asphalt mixes that are commonly used in Oklahoma. The study shows that the performance of each predictive model varies with the air voids and temperature of the test specimen. The Hirsch and the Al-Khateeb models were seen to perform with good accuracy at low temperatures. The Witczak 1999 and the Witczak 2006 models performed with good accuracy at high temperatures. None of the models performed well at low temperatures and high air voids. Calibration factors were developed at individual air voids levels to account for the inaccuracies in the model. It is anticipated that the use of calibration factors would be helpful in estimating dynamic modulus without conducting actual modulus tests in the laboratory. Moreover, the relationship between air voids and calibration factor is important to assist state agencies and pavement designers for Level 2 and Level 3 designs of the MEPDG for HMA mixes commonly used in Oklahoma.

5. A PROCEDURE TO ESTIMATE THE STIFFNESS OF AN ASPHALT PAVEMENT DURING CONSTRUCTION

5.1 INTRODUCTION

Verification of the quality of construction is as essential component of Quality Assurance (QA) function during the construction of Hot Mix Asphalt (HMA) pavements (Von Quintus et al., 2009; White and Thompson, 2008; Maupin, 2007; Akkinepally, 2006; Briaud and Seo, 2003). The accurate determination of the thickness and density of pavement, the mix parameters, and the comparison of these values with the design parameters are necessary in order to ensure the longevity of pavement. Quality Assurance (QA) and Quality Control (QC) programs provide the owner and contractor a means to ensure that the desired results are obtained to produce high-quality, long-life pavements. Desired results are those that meet or exceed the specifications and design requirements. Traditional pavement construction QA/QC procedures include a variety of laboratory and field test methods that measure volumetric and surface properties of pavement materials (Von Quintus et al., 2009).

QA procedures that are commonly used during the construction of asphalt pavements require the extraction of roadway cores from the finished pavement and may additionally require several measurements using a point-wise density measurement tool similar to a Nuclear Density Gauge (Zambrano et al., 2006). While the density measured from the cores provide an accurate indication of the quality, these tests are destructive in nature and are the source of some of the performance issues, such as potholes, that reduce the useful life of pavement (Maupin, 2007; Briaud and Seo, 2003). In addition, any quality issues that are identified during this process cannot be easily rectified after pavement has cooled down. Spot tests using nuclear or non-nuclear density gauges provide a quick measurement of the level of compaction, but have inherent limitations that reduce their effectiveness as QC methods. Furthermore, the above QC methods are time consuming to perform and are only helpful in determining the density of pavement layer at discrete number of points (Maupin, 2007; Briaud and Seo, 2003).

While the measurement of pavement density is a widely accepted method for acceptance testing for the finished pavement, such measurements are only an indirect measurement of the desired pavement property, namely pavement stiffness. Since pavement is designed to have adequate strength and stiffness to withstand the traffic load, the quantity of interest is stiffness of the finished pavement layers and not the density of pavement. As a result, there is an

emerging consensus that the stiffness of the asphalt pavement is a better indicator of the performance (Von Quintus et al., 2009; NCHRP, 2004).

The complexity of asphalt pavement compaction and the limitations of the spot tests have led researchers to develop advanced compaction technologies for improving the as-built quality of the pavements (Zambrano et al., 2006). Intelligent Compaction (IC) is a promising technology that can improve the quality of the road being constructed while reducing the associated cost and adverse environmental impacts. It provides a real-time complete coverage of the compaction area, and also reduces compaction costs resulting in significant overall construction cost saving (White et al. 2008; Maupin, 2007; Briaud and Seo, 2003; Zambrano et al., 2006; CTC, 2006; Singh et al., 2011; Commuri et al., 2009a, 2009b; Camargo et al., 2006; Peterson and Peterson, 2006; Petersen, 2005). As a result, several agencies in the United States have launched programs to evaluate the technology and determine the maturity of the technology for implementation (CTC, 2006).

Current research in Intelligent Compaction of HMA pavements demonstrates the application of continuous compaction control in order to achieve uniform compaction (FHWA, 2010). The development of techniques to measure dynamic modulus of asphalt mixtures over a wide range of temperatures and frequencies would be helpful in determining the quality of asphalt pavements during their construction. The estimation of stiffness in real-time will alleviate the quality control issues during the construction of HMA pavements. Further, mapping of the stiffness of the finished pavement will facilitate the acceptance testing of the constructed roadway.

The IACA functions on the hypothesis that the vibratory roller and the underlying pavement layers form a coupled system (Singh et al., 2011; Commuri et al., 2009a, 2009b). The response of the roller is determined by the frequency of its vibratory motors and the natural vibratory modes of the coupled system. Compaction of pavement increases its stiffness and as a consequence, the vibrations of the compactor are altered. The knowledge of the properties of the mat and the vibration spectra of the compactor can, therefore, be used to estimate compacted density or stiffness of the mat.

In this section, a procedure to estimate effective modulus of the pavement layer during construction is demonstrated. Given a location on the pavement, the estimated modulus of each of layer at this location is used to determine the effective modulus of the pavement layer. The

estimated modulus at this location can then be verified through Falling Weight Deflectometer (FWD) test. The FWD is currently the most common structural evaluation tool for the deflection-based NDT method (Abdallah et al., 2001). The method is non-destructive in nature and will help prevent under/over compaction of the asphalt pavement and achieve uniform compaction of the pavement.

5.2 BACKGROUND ON IACA

The functional modules in the IACA are schematically shown in Figure 5.1. The sensor module (SM) in the IACA consists of accelerometers for measuring the vibrations of the compactor during operation, infrared temperature sensors for measuring the surface temperature of the asphalt mat being compacted, and an user interface for specifying the amplitude and frequency of the vibration motors and for recording the mix type and lift thickness. The feature extraction (FE) module computes the Fast Fourier Transform (FFT) of the input signal and extracts the features corresponding to vibrations at different salient frequencies. The Neural Network (NN) Classifier is a multi-layer NN that is trained to classify the extracted features into different classes where each class represents a vibration pattern specific to a pre-specified level of compaction. The compaction analyzer (CA) then post-processes the output of the NN and estimates the degree of compaction in real time.

The first step in the use of the IACA during compaction in the field is the determination of the vibration features of the roller and their correlation with the compaction levels achieved. In order to accomplish this goal, a 30-meter long control strip is constructed first. The vibrations of the roller are measured using an accelerometer mounted on the axle of the drum. The power content in the vibration signals during each roller pass is then calculated, and the lowest and the highest power levels are determined (Singh et al., 2011; Commuri et al., 2009a, 2009b).

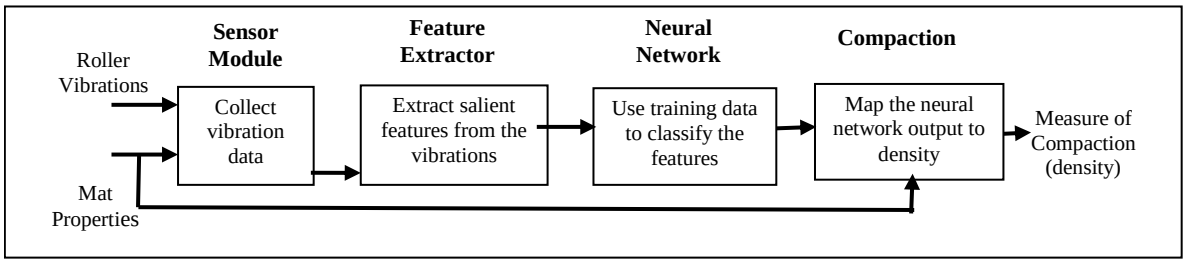

Figure 5.1 Functional schematic of the IACA

Five equally spaced power levels between the lowest and the highest power levels are identified and the features corresponding to these five power levels are used to train the NN.

During compaction, the NN observes the features of the roller vibration and classifies them into one of these five levels based on the levels of compaction that it is trained to recognize. Figure 5.2 shows typical features corresponding to the five different compaction levels extracted from the spectrogram of the vibration signals. In this figure, the lowest level corresponds to the case where the roller is operating with the vibration motors turned off, and the highest level corresponds to the case where the maximum vibrations are observed. It is assumed that the characteristics of the underlying pavement layers do not vary extensively over the project extent. That is, any changes in the spectra of the vibrations are a result of the compaction achieved in the topmost asphalt layer. In case the properties of the underlying layers are not constant, then the IACA will have to be periodically recalibrated. As a practical matter, large variations in the properties of the underlying pavement layers are usually a result of pavement failure or insufficient site preparation. Even if the IACA is not recalibrated, these effects result in low compaction even after several roller passes and can easily be detected.

After the IACA is trained to classify the vibrations into estimated levels of compaction, it is calibrated to reflect the modulus of pavement layer after construction. In order to accomplish this, dynamic modulus tests for the mix used in the construction of the asphalt mat are performed according to the AASHTO TP 62-03 test method (AASHTO, 2006). From the master curves, the modulus value (M_T) at the target density of the compacted mix (from the mix design sheet) is noted at selected temperature and frequency. This modulus value is assumed to be the highest modulus that can be achieved during the compaction of pavement. Likewise, the lowest modulus value observed, (M_{ld}), is assumed to correspond to the lay down density of the asphalt mat at same temperature and frequency. The modulus estimated by the NN model, (M_{NN}^{i}), at location $P_i\ (i=1,..,n)$, is then approximated as a linear relationship between stiffness of pavement and the observed levels of vibration.

$$M_{NN}^{i} = M_{ld} + k \times l_{NN}^{i} + off. \tag{5.1}$$

where, M^{i}_{NN} = modulus estimated by the neural network, k = slope, off = offset, and l^{i}_{NN} = compaction level estimated by the neural network. The initial slope is assumed to be equal to $(M_T - M_{ld})/$ (number of compaction levels), and the initial offset is set to zero.

The modulus estimated by the IACA after the initial calibration is based on the assumption that the target stiffness for the specified mix is indeed achieved during the compaction in the field. However, several factors such as the compaction equipment, rolling pattern, lay-down

temperature of the mix, lift thickness, etc., influence the actual modulus of pavement at any given location. In order to account for these deviations, measurements are taken using a FWD on the compacted pavement and the slope and offset in Eq. (5.1) are recalculated to minimize the error between the estimated and measured values. If the modulus measured at location P_i is represented by M^i_{FWD}, then the measurement error is given by e_i and can be calculated as

$$e_i = M^i_{NN} - M^i_{FWD} = M_{ld} + k \times l^i_{NN} + of\ \ f - M^i_{FWD}. \tag{5. 2}$$

Minimizing the mean square error (MSE), one obtains the desired slope '*k*'.

$$k = \frac{\sum_{i=1}^{n} \left[\left(M^i_{FWD} - M^i_{ld} - off \right) \times l^i_{NN} \right]}{\sum_{i=1}^{n} \left(M^i_{NN} \right)^2} \tag{5.3}$$

The new offset is calculated as the mean error between the estimated and the measured stiffness, that is

$$off = \frac{1}{n} \sum_{i=1}^{n} \left(M^i_{FWD} - M^i_{NN} \right) \tag{5.4}$$

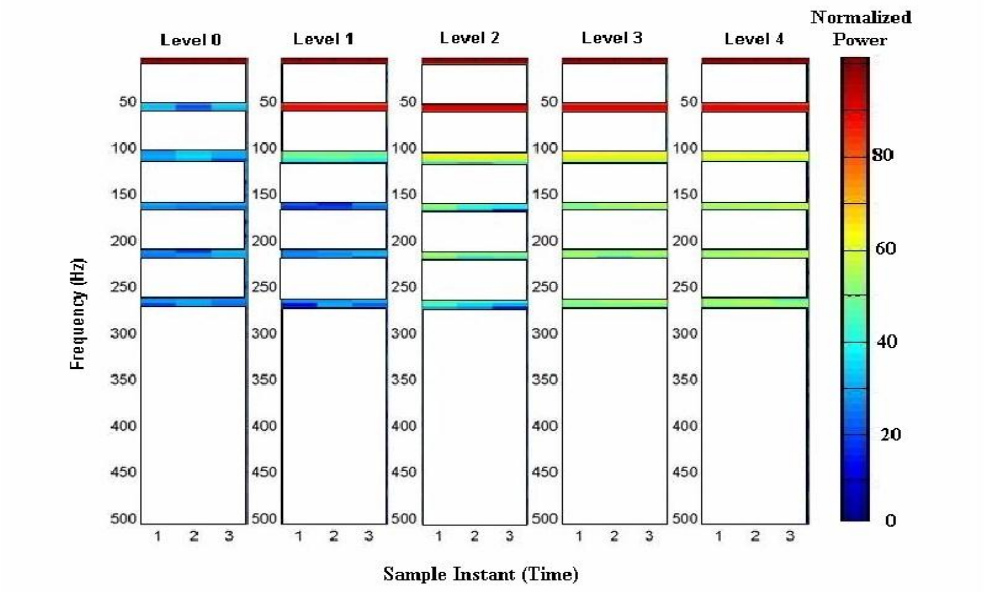

Figure 5.2 Spectral features corresponding to five levels of compaction

5.3 PROJECT DESCRIPTION

The use of the IACA in estimating the stiffness of a multi layer HMA pavement was investigated during the construction of Interstate I-35 in Norman, OK. This project involved the expansion of

the existing highway, stabilizing the subgrade to a depth of 200 mm using 10% cement kiln dust (CKD), followed by 200 mm thick aggregate base. The base layer was consisted of 100 mm thick asphalt layers of 19 mm Nominal Maximum Aggregate Size (NMAS) S3 (64-22 OK), while 2nd and 3rd layer were constructed with 19 mm NMAS S3 (76-28 OK) consisted of 100 mm and 75 mm thickness, respectively.

5.4 MEASUREMENT OF DENSITY USING THE IACA

The use of the IACA in estimating the stiffness of a three layers HMA pavement was investigated during the construction of Interstate I-35 in Norman, OK. A test section approximately 150 meters in length was selected and seven test locations, approximately 20 meters apart, were marked on the center line of the lane for verification analysis. The IACA was used to estimate the density of each of the layers during the construction. The IACA records the GPS coordinates of the roller in real time and the density estimated at this location during each roller pass.

The IACA was used to collect the GPS data and the density readings during the compaction of the all three layers (base, 2nd, and 3rd layers). First, the test points were marked on base layer, and the IACA data was collected. The GPS location of these points was recorded to locate these test locations on each pavement layer. Similar points were marked on 2nd and 3rd layers and the IACA data was collected during the compaction of each of these layers. The IACA data was analyzed to get the density estimate of each layers at all selected points. Previous research by authors concluded that The IACA measurements are typically within 1% of the density measured from pavement cores (Commuri et al., 2009a, 2009b). The measured density of each layer is given in Table 5.1. The density for base layer varies from 89.4% to 93.3%, similarly the density of 2nd and 3rd layers vary from 89.5% to 88.9%, and 91.8% to 93.3%, respectively. It can be seen that the density at each location changes with the layer type, with most consisent density being observed on the top layer. The density readings were converetd into air voids (% air voids = 100 -% density) and used to estimate dynamic modulus of each layer at the specified location. For example, if density of any spot is calculated as 96%, then the air voids of that particular location would be 4%. Now the dynamic modulus of this selected location was estimated from the master curves constructed for the given mix at a calculated air void levels (4 % air voids). The master curves are constructed at a wide range of the air voids to cover the air voids encountered in the field.

Table 5.1 IACA Measured Density of Each Layer

Test	IACA Estimated Density (%)		
Point	**Base Layer**	**2nd Layer**	**3rd Layer**
T8	**92.5**	**88.9**	**91.8**
T1N	**91.9**	**90.6**	**92.9**
T2N	**91.6**	**92.3**	**93.2**
T3N	**93.3**	**90.9**	**92.3**
T4N	**91.7**	**92.1**	**92.1**
T5N	**90.9**	**92.3**	**92.2**
M6	**89.4**	**89.5**	**93.3**

5.5 MATERIAL AND SPECIMEN PREPARATION

A loose HMA mixes of type S3 (PG 64-22 OK) and S3 (PG76-28) were collected from the construction site during the time of pavement construction. The S3 (PG 64-22) type of mix was used in base layer, while, S3 (PG 76-28) mix was used in 2nd and 3rd layers of pavement. The nominal maximum aggregate (primarily limestone) size for all mixes was 19 mm. The base mix contained approximately 20 percent 1" rock, 44 percent manufactured sand, 11 percent sand, and 25 percent recycled asphalt pavement (RAP), and 4.1 percent PG 64-22 OK binder. The 2nd and 3rd layer mixes contained approximately 22 percent 1" rock, 50 percent manufactured sand, 13 percent sand, and 15 percent recycled asphalt pavement (RAP), and 4.1 percent PG 76-28 OK binder. The gradations and other volumetric properties of all HMA mixes are given in Table 5.2 and Table 5.3, respectively. Loose HMA mixes were preheated in an oven, and specimens were compacted using a Superpave Gyratory Compactor (SGC). Three replicates of specimens were compacted at 6, 8, 10, and 12 % ± 1% target air voids levels. Initially, samples having 150 mm in diameter by 167.5 mm in height were prepared. Then, the test specimens of 100 mm in diameter were cored from the center of the gyratory compacted specimens, and sawed from each end of the specimen to get final sample of size 100 mm in diameter by 150 mm in height. The volumetric analysis was conducted to obtain effective binder content (V_{beff}), the voids in mineral aggregates (VMA), the voids filled with asphalt (VFA), and the air voids (V_a) for all the mixes (Table 5.4).

Table 5.2 Gradation of HMA Mixes

Material (%)	Base Layer	2nd and 3rd Layer
1" Rock	20	22
Manufactured Sand	44	50
Sand	11	13
RAP	25	15
Sieve Size (mm)	Gradation (% Passing)	
25	100	100
19	98	98
12.5	87	87
9.5	80	80
4.75	58	62
2.36	37	40
1.18	25	27
0.6	19	20
0.3	12	12
0.15	4	5
0.075	2.9	2.8

RAP = Reclaimed Asphalt Pavement

Table 5.3 Materials Volumetric Properties

		Base Layer	2nd and 3rd Layer
Volumetrics Properties			
G_{mm}		2.505	2.523
G_{se}		2.671	2.677
G_{sb}		2.645	2.657
G_b		1.01	1.01
Binder Type		PG 64-22	PG 76-28
P_b (%)		4.1	4.1
VMA (%)	Min.	14.1	14.81
	Max.	20.4	20
VFA (%)	Min.	39.9	41.9
	Max.	62.2	60.8
Va (%)		6, 8, 10, 12	
Aggregate Type		Limestone	Limestone
Mix Type		Recycled	Recycled

G_{mm} = Maximum Theoretical Specific Gravity Mixture

G_{sb} = Bulk Specific Gravity of Aggregate

G_{se} = Effective Specific Gravity of Aggregate

G_b = Specific Gravity of Binder

P_b = Asphalt Content

VMA = Voids in Mineral Aggregates

VFA = Voids Filled with Asphalt

V_a = Air Voids

Table 5.4 Specimens Volumetric Properties for HMA Mixes

		Base Layer (Mix- S3 64-22)			2nd and 3rd Layer (Mix S3 76-28)		
Target Air Voids (%)		Sample			Sample		
	(%)	1	2	3	1	2	3
6	V_a	5.4	5.6	5.6	6.5	6.4	6.4
	VMA	14.1	14.3	14.3	14.9	14.8	14.7
	VFA	62.2	61.4	61.5	60.1	60.4	60.8
	V_{beff}	8.8	8.8	8.8	8.9	8.9	9.0
8	V_a	7.3	7.2	7.2	8.3	8.1	7.9
	VMA	15.8	15.7	15.7	16.5	16.3	16.1
	VFA	54.5	54.7	54.9	53.3	53.9	54.6
	V_{beff}	8.6	8.6	8.6	8.8	8.8	8.8
10	V_a	9.3	9.6	9.1	9.6	10.2	9.8
	VMA	17.7	17.9	17.5	17.7	18.3	17.9
	VFA	47.7	46.9	48.3	48.9	47.0	48.3
	V_{beff}	8.4	8.4	8.4	8.6	8.6	8.6
12	V_a	11.5	12.4	12.4	12.2	11.7	12.0
	VMA	19.7	20.4	20.4	20.0	19.6	19.9
	VFA	41.8	39.9	39.9	41.9	43.2	42.3
	V_{beff}	8.2	8.1	8.1	8.4	8.4	8.4

V_a = Air Voids VMA = Voids in Mineral Aggregates
VFA = Voids Filled with Asphalt Vbeff = Effective asphalt content by volume

5.6 DYNAMIC MODULUS TESTING

Dynamic modulus was measured for all collected mixes at four different air voids: 6%, 8 %, 10%, and 12%. Dynamic modulus tests were performed using a MTS servo-hydraulic testing system. The test specimen was placed in an environmental chamber and allowed to equilibrium to the specified testing temperature ±0.5^{o}C. The specimen temperature was monitored using a dummy specimen with a thermocouple mounted at the center. Two linear variable differential transducer (LVDTs) were mounted on the specimen. Two friction reducing end treatment or teflon papers were placed between the specimen ends and loading plates. To begin testing, a minimal contact load was applied to the specimen. A sinusoidal axial compressive load was applied to the specimen without impact in a cyclic manner. The test was run on each test specimen at four different temperatures, namely, 4, 21, 40, and 55^{o}C, starting from the lowest temperature to the highest temperature. For each temperature level, the test was run at different frequencies from the highest to the lowest, namely, 25 , 10, 5, 1, 0.5, 0.1 Hz. Prior to testing, the sample was conditioned by applying 200 cycles of load at a frequency of 25 Hz. The load magnitude was adjusted based on the material stiffness, air void content, temperature, and frequency to keep the strain response within 50-150 micro-strains. The data was recorded for the last 5 cycles of each sequence. Dynamic modulus tests were performed according to the AASHTO TP62-03 (2006).

5.6.1 Development of Master Curves

Dynamic modulus of asphalt mixtures can be shifted along the frequency axis to form single characteristic master curves at a desired reference temperature or frequency. The master curve is generated at a reference temperature of 21^{o}C using the procedure outlined in Bonaquist et al., (2005). Equations (5.1) and (5.2) show the sigmoidal function and shift factor used for fitting the master curve. A nonlinear optimization program was used for simultaneously solving these unknown parameters.

$$\log|E^*| = \delta + \frac{(Max-\delta)}{1+e^{\beta+\gamma\left[\log(f)+c\left(10^{(A+VTS\log T_R)-\log\eta_{t=r}}\right)\right]}} \quad (5.1)$$

The shift factor used here was of the following form:

$$a(T) = \frac{f_r}{f} \quad (5.2)$$

where, Max is the maximum |E*| for a particular mix, f_r is the reduced frequency at reference temperature, f is the frequency at a particular temperature, $\eta_{t=r}$ is the viscosity of binder at reference temperature, A is the regression intercept of viscosity-temperature curve, VTS is the regression slope of viscosity-temperature susceptibility, $\alpha(T)$ is the shift factor as a function of temperature and age, and δ, β, γ, c are fitting parameters.

The A and VTS parameters for PG 64-22 (10.98, -3.680), and PG 76-28 (9.2, -3.024) were taken from the MEPDG guide (NCHRP, 2004). The constructed master curves for base, 2nd, and 3rd layers mixes are shown in Figure 5.3 and Figure 5.4, respectively. It can be seen from Figure 5.3, and Figure 5.4 that dynamic modulus value decreases as air voids increases. Developed master curves were then used to estimate dynamic modulus of each layers at given air voids, temperature, and frequency. The 'goodness-of-fit' statistic, S_e/S_y (standard error of the estimated/standard deviation), and correlation coefficient, (R^2), were used to assess the validity of the correlation between laboratory measured modulus and master curve fit equation (Odemark, 1949). Based on these criteria, the developed master curve equations in this study were found to be in excellent correlation with laboratory measured data. The coefficients and the fitting statistics of the master curves are summarized in Table 5.5.

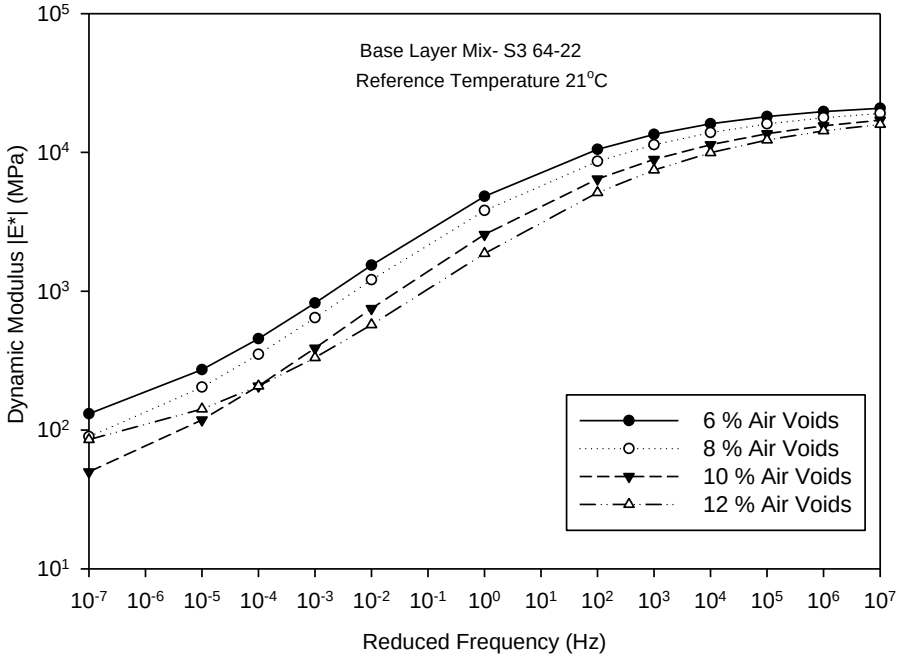

Figure 5.3 Master Curves for Base Layer Mixture (S3 64-22)

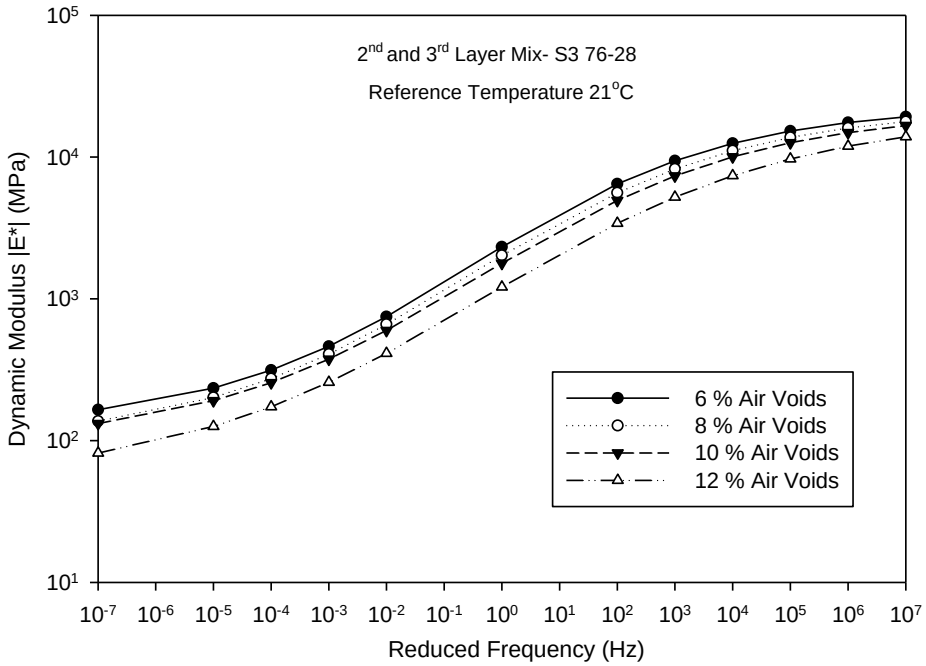

Figure 5.4 Master Curves for 2nd and 3rd Layers Mixtures (S3 76-28)

Table 5.5 Master Curves Parameters

Air Voids (%)	Max E* (MPa)	δ	β	γ	c	R^2	S_e/S_y	Fit
Base Layer (Mix- S3 64-22)								
6	23084	1.81	-1.02	-0.43	1.20	0.99	0.07	Excellent
8	22256	1.54	-0.98	-0.39	1.20	0.99	0.05	Excellent
10	21232	1.23	-0.86	-0.37	1.04	0.99	0.06	Excellent
12	19942	1.72	-0.41	-0.40	1.05	0.99	0.08	Excellent
2^{nd} and 3^{rd} Layer (Mix- S3 76-28)								
6	22826	2.10	-0.25	-0.45	1.24	0.99	0.04	Excellent
8	22027	1.99	-0.24	-0.42	1.18	0.99	0.05	Excellent
10	21157	1.98	-0.17	-0.42	1.12	0.99	0.04	Excellent
12	20182	1.71	-0.12	-0.37	1.13	0.99	0.05	Excellent

Shift Factors log(aT)

Air Voids (%)	Base Layer (Mix-S3 64-22)				2nd and 3rd Layer (Mix-S3 76-28)			
	4^o C	21^o C	40^o C	55^o C	4^o C	21^o C	40^o C	55^o C
6	2.66	0.00	-2.23	-3.60	2.24	0.00	-1.96	-3.20
8	2.65	0.00	-2.22	-3.58	2.13	0.00	-1.86	-3.04
10	2.30	0.00	-1.93	-3.11	2.02	0.00	-1.77	-2.89
12	2.32	0.00	-1.95	-3.14	2.04	0.00	-1.78	-2.91

5.7 ESTIMATING EFFECTIVE MODULUS OF PAVEMENT LAYERS

The FWD measured modulus is compared with the actual effective modulus of the layers using the Odemark method (Odemark, 1949) of equivalent thickness. The Odemark method is used to transform a system consisting of layers with different moduli into an equivalent system where the thickness of the layers are altered but all layers have the same modulus. The transformation assumes that the stiffness of the layer remains the same, i.e. $I \times E / (1 - \mu^2)$ remains constant where I = moment of inertia; E = layer modulus; and μ = Poisson ratio (Odemark, 1949; Huang, 2004; Ullidtz, 1998; Lytton, 1989).

This approach is used in the present study to calculate the effective modulus of the three layers that constitute the pavement on I-35. The IACA data collected during the compaction of each of the pavement layers was first used to determine density at selected locations. The estimated density (air voids) was then used to determine dynamic modulus at each of the each test locations. The effective modulus ($E_{effective}$) of three layers of pavement was calculated using

Equation 5.7. The effective moduli were calculated at 21^{o}C and 5 Hz (Table 5.6).The similar approach was used by several other researchers to find the effective modulus for layered system of pavement (Lu et al., 2009; Loulizi et al., 2007; Shalaby et al., 2004).

$$E_{effective} = \left[\frac{C_2\left(C_1 h_1 \sqrt[3]{E_1} + h_2 \sqrt[3]{E_2}\right) + h_3 \sqrt[3]{E_3}}{h_1 + h_2 + h_3}\right]^3 \quad (5.7)$$

E_1, E_2 and E_3 are dynamic modulus of 3rd (top layer), 2nd, and base layer, and h_1, h_2, and h_3 are the thickness of respective layers. C_1 and C_2 are the correction factors to obtain better agreement with exact theory of elasticity, (Ullidtz, 1998; Ullidtz and Peattie, 1980). The value of correction factors depend on the layer thicknesses, modular ratios, Poisson ratios and the number of layers in pavement structure. In the present study correction factors were taken as C_1 = 1.0 while C_2 = 0.8.

5.8 VERIFICATION OF EFFECTIVE MODULUS

The verification of the IACA measured modulus was done by conducting FWD testing on seven test locations that were marked before for estimating density using the IACA. The FWD is a non-destructive test device used to characterize the in-situ pavement moduli (Abdallah et al., 2001; Scullion, 2007). It drops a transient load from a specified height on a 300 mm diameter circular plate with a thin rubber pad mounted underneath. The load and deflection is measured using load cell and sensors set on the ground. Seven sensors were placed at 0, 200, 300, 450, 600, 900, and 1500 mm away from the center of the loading plate. In the present study the FWD test was conducted on 3rd layer of pavement using a Dynatest FWD test system. Numerical back-calculation software, MODULUS 6.0, was used to process the FWD raw data so as to determine the modulus value (Scullion and Liu, 2003). The backcalculated modulus is often called the effective modulus because the value represents the effect of the layer within the whole pavement structure. The effective modulus was calculated at 21^{o}C to compare this modulus with laboratory measured effective dynamic modulus. Since, the FWD loading induces a pulse of duration of 0.03 s (Loulizi et al., 2002), which is equivalent to a test frequency of 5.3 Hz (1/0.03/2π), hence, the comparisons in this paper are performed using modulus values calculated at 21^{o}C and 5 Hz frequency. Table 5.6 shows the results of the FWD test.

Table 5.6 Effective Modulus and FWD Modulus of Three Layers of Pavement

	Measured Dynamic Modulus (MPa)			Effective	FWD
Point	Base Layer	2nd Layer	3rd Layer	Modulus (MPa)	Modulus (MPa)
T8	5406	2190	3049	2365	3062
T1N	5070	2659	3456	2502	2482
T2N	4910	3227	3576	2637	2353
T3N	5889	2751	3227	2667	2696
T4N	4963	3155	3155	2554	2878
T5N	4556	3227	3191	2482	2657
M6	3880	2345	3617	2161	2760

5.9 RESULTS AND DISCUSSION

It is evident from Figure 5.5 that modulus estimated by the proposed method is in good agreement with the FWD measurements. However, the FWD readings show about 30% variation in the measured modulus for locations with identical density. Such reduction in the modulus values at certain locations might be due to variation in the subgrade, thickness of each layer, and inconsistency in the mix.

The ratio of FWD to effective modulus is shown in Figure 5.5. It can be seen that the ratio between the estimated modulus and the FWD measured modulus is close to 1. It is known from literature that 5% variation in FWD measured modulus is normally observed when repeated tests are performed at a given location (Gedafa et al., 2010; Hossain et al., 1992). Therefore, the error between the measured and estimated modulus is within the range of the measurement accuracy of the FWD device.

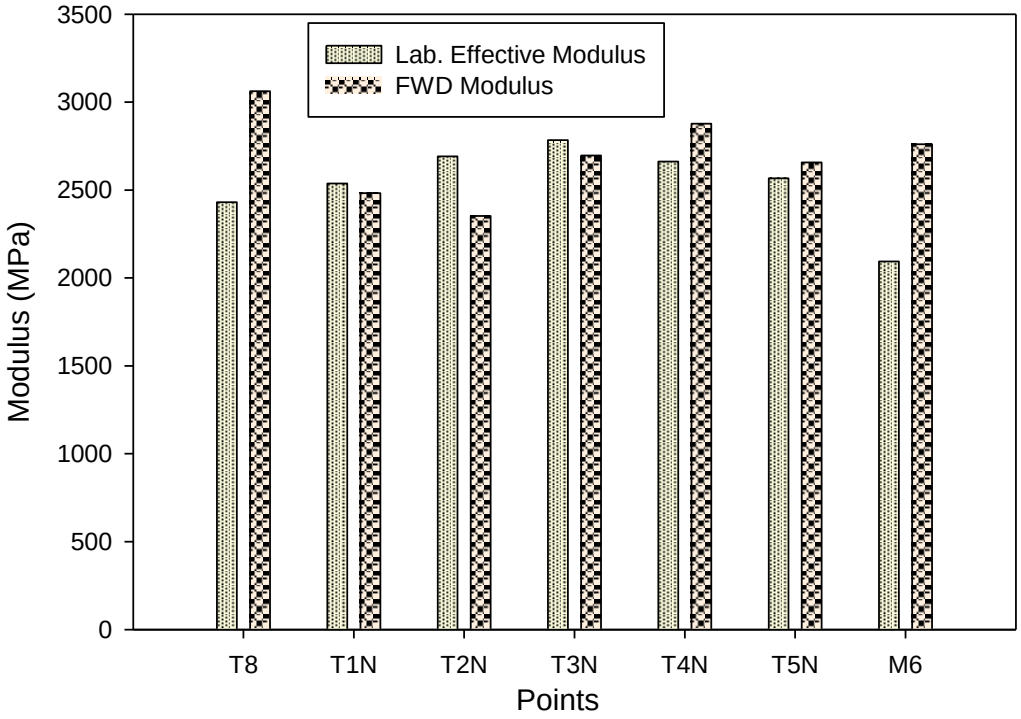

Figure 5.5 Comparison of Effective Modulus and FWD Modulus

5.10 OBSERVATIONS FROM THE STUDY

A neural network based Intelligent Asphalt Compaction Analyzer (IACA) to determine the stiffness of a pavement layer during it construction was demonstrated in this research project. The vibrations measured from the accelerometer equipped on the roller drum are used to determine the level of compaction that is achieved. These levels of compaction are then converted into a modulus value. The IACA provides the stiffness values over the entire pavement in a non-destructive manner.

Analyses of the results show that the proposed technique can accurately estimate the effective modulus of the pavement layers in real time during the construction process. Further, the accuracy of the measurements can be independently verified using a Falling Weight Deflectometer. The method is non-destructive in nature and will help prevent under/over compaction of the asphalt pavement and achieve uniform compaction of the pavement. Research is currently underway to validate the performance of the IACA during the compaction of Warm Mix Asphalt pavements and during the compaction of stabilized soil subgrades.

6. CONCLUSIONS AND DIRECTION OF FUTURE RESEARCH

6.1 CONCLUSIONS

The extension of the Intelligent Asphalt Compaction Analyzer technology for the estimation of the stiffness of asphalt pavements during their construction was addressed in this study. The dependence of the dynamic modulus of compacted asphalt specimens on mix properties, temperature, loading frequency etc., was first studied in the laboratory. The results of the laboratory study were used to specify the target modulus value for each pavement layer during the construction. These values were then used to develop automated procedures for the calibration of the IACA during the construction of asphalt pavements. The accuracy and repeatability of the IACA in estimating the pavement modulus were demonstrated during the construction of multi-layered asphalt pavement. The following are the results of the research study.

- The Dynamic Modulus of the asphalt mix is a viable candidate for specifying the stiffness of asphalt pavements. Further, the modulus measured in the laboratory for a given asphalt mix can be easily correlated with the modulus measured in the field through Falling Weight Deflectometer (FWD) tests.

- Empirical models can be used to determine the stiffness of a compacted asphalt specimen. However, correction factors for the empirical models have to be developed prior to their use in order to avoid over/under prediction of the modulus.

- The IACA can be used to obtain estimates of the stiffness of the pavement during the compaction. The estimates are obtained in real-time and are indicative of the properties of the overall pavement. Such estimates can be used to detect under compacted areas and well compacted areas on the pavement. Such information can be used by the roller operator to address under compaction while the asphalt mix is still hot and pliable while avoiding over compaction of the mix.

- The as-built maps generated by the IACA include the estimated stiffness over the entire pavement along with the GPS coordinates of each location. These maps will help in the

quality assurance / acceptance testing of the completed pavement and could also serve as a vital record of the quality of the construction.

- The IACA prototype is rugged, easy to use, and of the accuracy necessary for its use as a QC tool in the compaction of asphalt pavements. The IACA can also be used as a drop-in replacement for retrofitting existing vibratory compactors.

- Several utilities for analyzing the quality of the compaction were implemented in the IACA software. These utilities directly aid the contractor in obtaining uniformity in compaction and increasing the productivity. Specifically, the built-in features allow the operator to check coverage and rolling patterns; investigate pass-by-pass variations in stiffness of the pavement; monitor the temperature profile of the surface of the asphalt mat; and generate as-built maps and statistical estimates of the overall compaction.

6.2 COLLABORATIVE PARTNERSHIPS AND TECHNOLOGY TRANSFER

The extension of the Intelligent Asphalt Compaction Analyzer (IACA) to the estimation of the stiffness of asphalt pavements during their construction was undertaken between June 2009 and October 2010 through the financial support of the Oklahoma Transportation Center and Volvo Construction Equipment, Shippensburg, PA. The IACA technology is licensed to Volvo Construction Equipment Company (VCE) which is not only manufacturing the IACA but is also partnering with OU to extend this technology to the compaction of soil subgrades. VCE is excited at this technology and has structured their high-end compaction technologies around the IACA. VCE has entered into exclusive licensing agreement with OU for the IACA technology and is committed to sponsoring this research. This collaboration has resulted in additional leveraged funding of $831,119 over this same period.

The results achieved in this project demonstrate the importance of teamwork and successful collaborations in developing innovative solutions to mitigate long-standing quality issues during the construction of asphalt pavements. The project team benefited from its close technical cooperation with the Oklahoma Department of Transportation (ODOT), asphalt contractors (Haskell Lemon Construction Company, Oklahoma City), Equipment Manufacturer (Volvo Construction Equipment, Shippensburg, PA), and test companies (Burgess Engineering, Moore, OK). Having access to the technical expertise at Volvo Construction Equipment Company enabled the team to put together reliable, production-ready solutions in a cost-effective manner. Having ready access to construction sites (Haskell Lemon Construction Company) and material testing facilities (Burgess Engineering) has enabled the rigorous testing of the IACA and contributed to the development of a “fail safe” and rugged IACA prototype.

6.3 FUTURE OPPORTUNITIES AND CHALLENGES

The results of this study and the ongoing demonstration clearly show that the IC technology is mature and can address several of the quality issues faced by the contractor during the construction of asphalt pavements. Several of these quality issues can be traced back to the lack of adequate tools for QC during the construction process. The IACA technology can not only rectify this problem, but can also provide complete documentation of the quality of the constructed pavement. Improved QC will have the immediate effect of increasing the longevity of pavements and reducing the cost of their construction and maintenance. While competing technologies require the purchase of a new vibratory compactor equipped with IC technology,

the IACA can be retrofitted on any vibratory compactor.

The extension of IACA to compaction of stabilized soils is currently underway under support from Oklahoma Transportation Center (OTCREOS 10.1-11) and Volvo Construction Equipment, Shippensburg, PA. Rigorous field testing of the stiffness measurements for asphalt pavements is being carried out at multiple locations in Oklahoma during 2011-2012 with support from VCE. The research team is also actively pursuing closed-loop continuous compaction control to guarantee adequate compaction of soil subgrades and pavement layers. The research team has put in place a multi-year research program with the assistance of VCE to meet these long term objectives.

While the market has been ready for IC technology for several years, several challenges need to be met before the technology can be successfully integrated into the workspace. The primary challenges that the research team encountered during the course of this study are listed below:

- Lack of clear acceptance specifications. Current acceptance specifications require the extraction of roadway cores as a part of the acceptance testing. The pay factors are also calculated based on the density measured from the extracted cores. Thus, the asphalt contractor is still bound by existing specifications and does not perceive the need for IC-based quality testing.

- Lack of incentives for the use of IC technology. While the use of IACA to determine the uniformity of compaction and prevent over- and under-compaction of asphalt mats has been demonstrated, the cost savings and the increase in productivity that can be obtained have not been adequately recognized by the user community. The primary reason is that roller operators and their supervisors are entirely focused on the traditional methods of construction, and there is a noticeable averseness to risks associated with newer technologies. This can be a significant impediment to the integration of IC technologies into construction practices unless the contractors are incentivized to use IC technologies.

- Need for outreach and education. The research team routinely encountered reluctance on the part of the user community due to the perception that (a) new technology is risky; (b) new technologies require exceptional literacy and computer skills and in the long

term cause job attritions. While the IC demonstrations address this aspect to some extent, there is still a need for significant outreach and training, from the construction crew all the way up to the State and Federal agencies that oversee the construction of this critical infrastructure.

REFERENCES

1. Abdallah, I., Yuan, D., and Nazarian, S. Integrating Seismic and Deflection Methods to Estimate Pavement Moduli. Journal of Transportation Research Record, No. 1755, 2001, pp. 43-50.
2. Abdo, A.A., Bayomy, F., Nielsen, R., Weaver, T., and Jung, S.J. Prediction of the Dynamic Modulus of Superpave Mixes. Bearing Capacity of Roads, Railways and Airfields, pp. 305-314, 2009.
3. Akkinepally, R. Quality Control and Quality Assurance of Hot Mix Asphalt Construction in Delaware. Master's Thesis, University of Delaware, Newark, 2006.
4. Al-Khateeb, G., Shenoy, A., Gibson, N., and Harman, T. A new simplistic model for dynamic modulus predictions of asphalt paving mixtures. Journal of the Association of Asphalt Paving Technologists, Vol. 75, 2006, pp. 1254–1293.
5. American Association of State Highway and Transportation Officials (AASHTO): Standard Method of Test for Bulk Specific Gravity of Compacted Bituminous Mixtures Using Saturated Surface Dry Specimens: T166, 2006.
6. American Association of State Highway and Transportation Officials (AASHTO). Standard Method of Test for Determining Dynamic Modulus of Hot-Mix Asphalt Concrete Mixtures: TP62-03. AASHTO Provisional Standards, 2006.
7. American Society for Testing and Materials (ASTM). Viscosity-Temperature Chart for Asphalt. Annual Book of ASTM Standards, Vol. 0.0403, 2009.
8. Andrei, D., Witczak, M.W., Mirza, M.W. Development of a Revised Predictive Model for the Dynamic (Complex) Modulus of Asphalt Mixtures, NCHRP 1-37A Interim Team Report, University of Maryland, March 1999.
9. Azari, H., Al-Khateeb, G., Shenoy, A., and Gibson, N. Comparison of Simple Performance Test |E*| of Accelerated Loading Facility Mixtures and Prediction |E*| use of NCHRP 1-37 A and Witczak's New Equations. Transportation Research Record, No. 1998, TRB, 2007, pp. 1-9.
10. Bari, J., and Witczak, M.W. Development of a New Revised Version of the Witczak E* Predictive Model for Hot Mix Asphalt Mixtures. Journal of the Association of Asphalt Paving Technologists, Vol. 75, 2006, pp. 381-423.
11. Bari, J., and Witczak, M.W. New Predictive Models for Viscosity and Complex Shear Modulus of Asphalt Binders for Use with Mechanistic-Empirical Pavement Design Guide. Transportation Research Record, No. 2001, TRB, 2007, pp. 9-19.

12. Birgisson, B., Sholar, G., and Roque, R. Evaluation of a Predicted Dynamic Modulus for Florida Mixture. Transportation Research Record, No. 1929, TRB, 2005, pp. 200-207.
13. Bonaquist, R., and Christensen, D.W. Practical Procedure for Developing Dynamic Modulus Master Curves for Pavement Structural Design. Transportation Research Record: Journal of Transportation Research Board, No. 1929, 2005, pp. 208-217.
14. Briaud, J. L., and Seo, J. Intelligent Compaction: Overview and Research Needs. Texas A&M University, College Station, 2003.
15. Camargo, F., Larsen, B., Chadbourn, B., Roberson, R., and Siekmeier, J. Intelligent Compaction: A Minnesota Case History. 54th Annual University of Minnesota Geotechnical Conference, 2006.
16. Ceylan, H., Gopalakrishnan, K., and Kim, S. Advanced Approached to Hot Mix Asphalt Dynamic Modulus Prediction. Canadian Journal of Civil Engineering, Vol. 35, 2008, pp. 699-707.
17. Ceylan, H., Schwartz, C.W., Kim, S., and Gopalakrishnan, K. Accuracy of Predictive Models for Dynamic Modulus of Hot Mix Asphalt. ASCE Journal of Materials in Civil Engineering, Vol. 21, No. 6, 2009, pp. 286-293.
18. Chehab, G., O'Quinn, R. E., and Kim, Y. R.(2000) Specimen Geometry Study for Direct Tension Test Based on Mechanical Tests and Air Void Variation in Asphalt Concrete Specimens Compacted by Superpave Gyratory Compactor. Journal of Transportation Research Record, No. 1723, 2000, pp. 125–132.
19. Christensen, D.W., Pellinen, T., and Bonaquist, R.F. Hirsch model for estimating the modulus of asphalt concrete. Journal of the Association of Asphalt Paving Technologists, Vol. 72, 2003, pp. 97–121.
20. Cominsky, R.J., Killingsworth, B.M., Anderson, R.M., Anderson, D.A., and Crockford, W.W. (1998). Quality control and acceptance of superpave designed hot mix asphalt. Project D9-7, NCHRP Report No. 409, Transportation Research Board, Washington, D.C.
21. Commuri, S., Mai, A., and Zaman, M. Calibration Procedures for the Intelligent Asphalt Compaction Analyze. ASTM Journal of Testing and Evaluation, vol. 37, no. 5, 2009a, pp. 454-462.
22. Commuri, S., Mai, A., and Zaman, M. Neural Network-based Intelligent Compaction Analyzer for Estimating Compaction Quality of Hot Asphalt Mixes. ASCE Journal of Construction Engineering and Management, 2009b (accepted for publication).

23. CTC. Intelligent Compaction of Soils." CTC and Associates LLC and WisDOT Research and Communication Services Wisconsin Highway Research Program, Wisconsin, 2006.
24. Daniel, J. S.(2001). Development of a Simplified Fatigue Test and Analysis Procedure Using a Viscoelastic, Continuum Damage Model and Its Implementation to WesTrack Mixtures. Ph.D. dissertation. North Carolina State University, Raleigh.
25. Dongre, R., Myers, L., D'Angelo, J., and Gudimettla, J. Field Evaluation of Witczak and Hirsch Models for Predicting Dynamic Modulus of Hot-Mix Asphalt. Journal of the Association of Asphalt Paving Technologists, Vol. 74, 2005.
26. Far, M.S.S., Underwood, B.S., Ranjithan, S.R., Kim, Y.R., and Jackson, N. Application of Artificial Neural Networks for Estimating Dynamic Modulus of Asphalt Concrete. Transportation Research Record, No. 2127, TRB, 2009, pp. 173-186.
27. FHWA (2005). "Highway Statistics 2005, Providing information to address major transportation issues facing the Nation." Office of Highway Policy Information, Federal Highway Administration, Washington. D.C.
28. FHWA (2006). "Highway Statistics 2005." Federal Highway Administration, Washington, D.C.
29. FHWA (2007). "National Asphalt Roadmap**,** Asphalt Pavement Research and Technology, A Special Report by Federal Highway Administration," *Draft: Second Report,* Washington D.C.
30. FHWA (2011). Federal Highway Administration. Intelligent Compaction. www.intelligentcompaction.com (Last accessed May 15, 2011).
31. Gedafa, D.S., Hossain, M. , Romanoschi, S.A., and Gisi, A.J. Comparison of Moduli of Kansas Superpave Asphalt Mixes. 89th Annual Transportation Research Board Meeting, Washington, D.C., 2010.
32. Goh, S.W., You,Z., Williams, R.C., and Li, Xinjun. (2011). Preliminary Dynamic Modulus Criteria of HMA for Field Rutting of Asphalt Pavements: Michigan's Experience. ASCE, Journal of Transportation Engineering, Vol. 137, No.1, pp.37-45.
33. Hossain, M., and Scofield, L. Correlation Between Backcalculated and Laboratory-Determined Asphalt Concrete Moduli. Journal of Transportation Research Record, No. 1377,1992, pp. 67-76.
34. Huang, Y. Pavement Analysis and Design." Pearson Prentice Hall, NJ, 2004, pp. 124-125.
35. Kim, Y.R., King, M., and Momen, M. Typical Dynamic Moduli Values of Hot Mix Asphalt in North Carolina and Their Prediction. CD-ROM. 84th Annual Meeting, TRB, 2005.

36. Loulizi, A., Al-Qadi, I.L., Lahouar, S., and Freeman, T. Measurement of Vertical Compressive Stress Pulse in Flexible Pavements and Its Representation for Dynamic Loading. Presented at the Transportation Research Board 81st Annual Meetings Paper # 02-2376, Washington, D.C., 2002, pp. 1-21.
37. Loulizi, A., Flintsch, G.W., and McGhee, K. Determination of in-Place Hot-Mix Asphalt Layer Modulus for Rehabilitation Projects by a Mechanistic-Empirical Procedure. Transportation Research Record,, No. 2037, TRB, 2007, pp. 53-62.
38. Lu, Q., Ullidtz, P., Basheer, I., Ghuzlan, K., and Signore, J.M. CalBack: Enhancing Caltrans Mechanistic-Empirical Pavement Design Process with New Back-Calculation Software. Journal of Transportation Engineering, Vol. 135, No.7, 2009, pp. 479-488.
39. Lytton, R. Backcalculation of Pavement Layer Properties. ASTM, STP 1026: Nondestructive Testing of Pavements and Backcalculation of Moduli, 1989, pp. 14-15.
40. Maupin, G. W. Preliminary Field Investigation of Intelligent Compaction of Hot-Mix Asphalt. Virginia Transportation Research Council, Charlottesville, 2007.
41. Moretti, M. (2005). "Rough Roads," TRIP – a Transportation Research Group, http://www.tripnet.org/national/RoughRoadsPR052605.htm
42. NCHRP, American Association of State Highway and Transportation Officials (AASHTO). Guide to the Mechanistic-Empirical Design of New and Rehabilitated Pavement Structures. Washington, D.C. 2004. http://www.trb.org/mepdg/guide.htm.
43. OAPA (2003). "Key Facts about Oklahoma's Road and Bridge Conditions and Federal Funding." Oklahoma Asphalt Pavement Association (OAPA), Oklahoma City, Oklahoma.
44. Obulareddy, S. Fundamental Characterization of Louisiana HMA Mixtures for the 2002 Mechanistic-Empirical Design Guide. Master's Thesis, Louisiana State University, 2006.
45. Odemark, N. Investigations as to the Elastic Properties of Soils Design of Pavement According to the Theory of Elasticity. Staten Vaeginstitut, Stockholm, Sweden, 1949.
46. Pellinen, T.K., and Witczak, M.W. Use of Stiffness of Hot-Mix Asphalt as a Simple Performance Test. Journal of Transportation Research Board, No. 1789, 2002, pp. 80-90.
47. Petersen, D. L. Continuous Compaction Control MnROAD Demonstration. Minnesota Department of Transportation, Maplewood, 2005.
48. Peterson, L., and Peterson, R. Compaction and In-Situ Testing at Mn/DOT TH53. Minnesota Department of Transportation, St. Paul, 2006.

49. Schwartz, C. Evaluation of the Witczak Dynamic Modulus Prediction Model. CD-ROM. 84th Annual Meeting, TRB, 2005.
50. Schwartz, C. W., Gibson, N., and Schapery, R. A. (2002). Time–Temperature Superposition for Asphalt Concrete at Large Compressive Strains. Journal of Transportation Research Record No. 1789, pp. 101-112.
51. Scullion, T. Perpetual Pavements in Texas: The State of the Practice. Technical Report FHWA/TX-05/0-4822-1, Texas Transportation Institute, College Station, Texas, 2007.
52. Scullion, T., and Liu, W. Modulus 6.0 for Window: User's Manual. Technical Report 0-1869-2, TT, College Station, Texas, 2003.
53. Shalaby, A., Liske, T., and Kavussi, A. Comparing Back-Calculated and Laboratory Resilient Moduli of Bituminous Paving Mixtures. Canadian Journal of Civil Engineering, Vol. 31, 2004, pp. 988-996.
54. Shenoy, A., and Romero, P. (2002). Standardized procedure for analysis of dynamic modulus (E*) data to predict asphalt pavement distresses. Transportation Research Record, No. 1789, pp. 173-182.
55. Singh, D.V., Mai, A.T., Beainy, A.F., Commuri, S., and Zaman, M.M. In-situ Assessment of Stiffness during the Construction of HMA Pavements. International Journal of Pavement Research and Technology, Vol.4, Issue: 3, 2011, pp. 131-139.
56. Tran, N.H., and Hall, K.D. (2006). An Examination of strain levels used in the dynamic modulus testing. Journal of Association of Asphalt Paving Technologist, Vol. 75, pp. 321-343.
57. Tran, N.H., and Hall, K.D. Evaluating the Predictive Equation in Determining Dynamic Moduli of Typical Asphalt Mixtures Used in Arkansas. Journal of the Association of Asphalt Paving Technologists, Vol. 74, 2005, pp. 1-17.
58. Ullidtz, P. Modeling Flexible Pavement Response and Performance. Narayana Press, Odder, Denmark, 1998, pp. 38-43.
59. Ullidtz, P., and Peattie, K. R. Pavement Analysis by Programmable Calculators. Journal of the Transportation Engineering, ASCE, Vol. 106, 1980, No. TE5, pp. 581-597.
60. Von Quintus, H.L., Rao, C., Ninchin, R.E., Nazarian, S., and Prowell, B. NDT Technology for Quality Assurance of HMA Pavement Construction. National Cooperative Highway Research Program, Report No. 626, 2009.
61. White, D. J., and Thompson, M. J. Relationships between In Situ and Roller-Integrated Compaction Measurements for Granular Soils. Journal of Geotechnical and Geo-environmental Engineering, Vol. 134, No. 12, 2008, pp. 1763-1770.

62. Witczak, M., Kaloush, K., and Von Quintus, H. (2002). Pursuit of the Simple Performance test for asphalt mixture rutting. Journal of the Association of Asphalt Paving Technologies, Vol. 71, pp. 671-691.
63. Witczak, M.W, Kaloush, K., Pellinen, T., El-Basyouny, M., and Quintus, H. Simple Performance Test for Superpave Mix Design, NCHRP Report 465, 2002.
64. Zambrano, C., Drnevich, V., and Bourdeau, P. Advanced Compaction Quality Control. Indiana Department of Transportation, Indianapolis, 2006.